USGS
science for a changing world

Prepared in cooperation with the Bureau of Land Management

Hierarchical Population Monitoring of Greater Sage-Grouse (*Centrocercus urophasianus*) in Nevada and California—Identifying Populations for Management at the Appropriate Spatial Scale

Open-File Report 2017–1089

U.S. Department of the Interior
U.S. Geological Survey

Cover: Photograph of a male greater sage-grouse performing a courtship display on a lek south of Wells, northeastern Nevada, 2012. Photograph courtesy of Tatiana Gettelman.

Hierarchical Population Monitoring of Greater Sage-Grouse (*Centrocercus urophasianus*) in Nevada and California—Identifying Populations for Management at the Appropriate Spatial Scale

By Peter S. Coates, Brian G. Prochazka, Mark A. Ricca, Gregory T. Wann, Cameron L. Aldridge, Steve E. Hanser, Kevin E. Doherty, Michael S. O'Donnell, David R. Edmunds, and Shawn P. Espinosa

Prepared in cooperation with the Bureau of Land Management

Open-File Report 2017–1089

U.S. Department of the Interior
U.S. Geological Survey

U.S. Department of the Interior
RYAN K. ZINKE, Secretary

U.S. Geological Survey
William H. Werkheiser, Acting Director

U.S. Geological Survey, Reston, Virginia: 2017

Suggested citation
Coates, P.S., Prochazka, B.G., Ricca, M.A., Wann, G.T., Aldridge, C.L., Hanser, S.E., Doherty, K.E., O'Donnell, M.S., Edmunds, D.R., and, Espinosa, S.P., 2017, Hierarchical population monitoring of greater sage-grouse (*Centrocercus urophasianus*) in Nevada and California—Identifying populations for management at the appropriate spatial scale: U.S. Geological Survey Open-File Report 2017-1089, 49 p., https://doi.org/10.3133/ofr20171089.

ISSN 2331-1258 (online)

Preface

This study was conducted to provide timely scientific information to establish an adaptive monitoring framework and modeling approach for greater sage-grouse (*Centrocercus urophasianus*) population trends at multiple spatial scales in northeastern California and Nevada. These findings fill a prominent information gap, and heighten understanding of sage-grouse population trends at nested spatial and temporal scales. Importantly, this study highlights an example of an 'early warning system' that can be carried out annually to identify where and when management action could be applied to benefit declining populations of sage-grouse at the appropriate scale. The rules of this framework can be modified to identify populations responding positively to management actions, and could ultimately be implemented across the geographic range of sage-grouse. This report is also intended to provide timely scientific information and inform newly established State and Federal monitoring programs, particularly those of the Bureau of Land Management and U.S. Forest Service.

Acknowledgments

This project was conducted in close consultation with the Bureau of Land Management (BLM), Nevada Department of Wildlife (NDOW), U.S. Forest Service (USFS), U.S. Fish and Wildlife Service (FWS), Colorado State University, and California Department of Fish and Wildlife (CDFW). We thank M. Magaletti, A. Kosic, P. Winters (BLM), J. Tull (NDOW), K. Borland, M. Nelson (USFS), S. Abele (USFWS), and B. Ehler (CDFW) for their input throughout the development of the project. We greatly appreciate the cooperation of NDOW and CDFW for providing lek survey data. We also extend particular gratitude to T. Remington (Western Association of Fish and Wildlife Agencies) for executing quality assurance and quality control procedures for all lek data used in the signal analysis. Reviews of previous manuscript drafts by A. Duarte (Oregon State University), Jonathan Rose (USGS), A. Monroe (Colorado State University), and T. Kimball (USGS) were particularly helpful. We thank M. Chenaille and C. Roth (USGS) for assistance with GIS analyses, and J. Atkinson (USGS) for help with report preparation.

Contents

Figures

Tables

Conversion Factors

International System of Units to U.S. customary units

Multiply	By	To obtain
	Length	
meter (m)	3.281	foot (ft)
kilometer (km)	0.6214	mile (mi)
	Area	
hectare (ha)	2.471	acre
square hectometer (hm^2)	2.471	acre
square kilometer (km^2)	0.3861	square mile (mi^2)
square kilometer (km^2)	247.1	acre

Datums

Vertical coordinate information is referenced to the North American Vertical Datum of 1988 (NAVD 88).
Horizontal coordinate information is referenced to the North American Datum of 1983 (NAD 83).
Elevation, as used in this report, refers to distance above the vertical datum.

Hierarchical Population Monitoring of Greater Sage-Grouse (*Centrocercus urophasianus*) in Nevada and California—Identifying Populations for Management at the Appropriate Spatial Scale

By Peter S. Coates[1], Brian G. Prochazka[1], Mark A. Ricca[1], Gregory T. Wann[1], Cameron L. Aldridge[1,2], Steve E. Hanser[1], Kevin E. Doherty[3], Michael S. O'Donnell[1], David Edmunds[1,2], and Shawn P. Espinosa[4]

Abstract

Population ecologists have long recognized the importance of ecological scale in understanding processes that guide observed demographic patterns for wildlife species. However, directly incorporating spatial and temporal scale into monitoring strategies that detect whether trajectories are driven by local or regional factors is challenging and rarely implemented. Identifying the appropriate scale is critical to the development of management actions that can attenuate or reverse population declines. We describe a novel example of a monitoring framework for estimating annual rates of population change for greater sage-grouse (*Centrocercus urophasianus*) within a hierarchical and spatially nested structure. Specifically, we conducted Bayesian analyses on a 17-year dataset (2000–2016) of lek counts in Nevada and northeastern California to estimate annual rates of population change, and compared trends across nested spatial scales. We identified leks and larger scale populations in immediate need of management, based on the occurrence of two criteria: (1) crossing of a *destabilizing threshold* designed to identify significant rates of population decline at a particular nested scale; and (2) crossing of *decoupling thresholds* designed to identify rates of population decline at smaller scales that decouple from rates of population change at a larger spatial scale. This approach establishes how declines affected by local disturbances can be separated from those operating at larger scales (for example, broad-scale wildfire and region-wide drought). Given the threshold output from our analysis, this adaptive management framework can be implemented readily and annually to facilitate responsive and effective actions for sage-grouse populations in the Great Basin. The rules of the framework can also be modified to identify populations responding positively to management action or demonstrating strong resilience to disturbance. Similar hierarchical approaches might be beneficial for other species occupying landscapes with heterogeneous disturbance and climatic regimes.

[1]U.S. Geological Survey.
[2]Colorado State University.
[3]U.S. Fish and Wildlife Service.
[4]Nevada Department of Wildlife.

Synopsis

Monitoring strategies for species of concern can be made more powerful by taking advantage of recent advances in ecological models that account for differences in population dynamics across spatial and temporal scales. It is critical to identify the scale where populations are changing (for example, local compared to regional) so that management actions designed to ameliorate population declines may be applied effectively. Here, we describe a novel example of a hierarchical and spatially nested monitoring framework for estimating annual rates of population change (λ) for greater sage-grouse (*Centrocercus urophasianus*) as an early warning system for detecting significantly declining populations. Using a reductionist approach, this framework establishes the relevance of spatial and temporal scales, and the direction and magnitude of population changes across space and time. First, the framework allows partitioning of local compared to regional effects that are likely to influence populations adversely, which can then help identify the appropriate scale to target actions aimed at reversing such effects. Second, the framework incorporates temporal thresholds, whereby multiple years of decline must occur before management action is initiated, which guards against transient demographic stochasticity or erroneous lek counts during a particular year. Third, the framework quantifies the duration and magnitude of decline at the identified spatial scale to help inform where and when to apply appropriate management actions. Accordingly, steady or precipitous declines governed by local disturbances that are more manageable (for example, wildfire, inappropriate grazing, energy development) are separated from those operating at larger spatial scales that are less manageable (for example, region-wide drought).

Our monitoring framework example focuses on sage-grouse populations in Nevada and northeastern California. We first partitioned sage-grouse lek locations into lek clusters across multiple spatially nested, hierarchical scales based on landscape and climatic characteristics influencing spatial connectivity among sage-grouse populations. This analysis indicated three tractable scales for use in our example—individual lek, a neighborhood cluster, and a climate cluster. Using 17 continuous years of annual lek count data (2000–2016), we estimated annual rates of population change by fitting state-space models in a Bayesian statistical framework. Using these estimates, we initiated a three-step evaluation process at the nested spatial scales to identify declining populations: *thresholds, warnings,* and *signals*. The evaluation process stops if any criteria at any step are not met.

For step 1, we used a retrospective simulation analysis to estimate two types of *thresholds* describing population declines: (1) *destabilizing* thresholds designed to identify significant rates of population decline at a particular nested scale; and (2) *decoupling* thresholds aimed at identifying when the rates of population decline at a local scale (for example, individual leks and neighborhood clusters, where management may be effective) detrend significantly from median rates of population change at a larger spatial scale (for example, climate clusters, where large-scale variations in climate can drive population cycles of sage-grouse, and are therefore less manageable by direct intervention). We further differentiated between the rates (*slow* and *fast*) at which a population can cross a threshold. This rate establishes the magnitude of population change within the monitoring framework. A *slow* threshold indicates slow rates of decline and decoupling, whereas a *fast* threshold indicates more precipitous rates of decline and decoupling. For step 2, a slow or fast *warning* activates if both destabilizing and decoupling thresholds are crossed. For step 3, crossing of a temporal threshold (that is, a sequence of annual warnings) specifies whether to activate a *soft* or *hard signal*. Based on results of post-hoc simulation analysis (described in the paragraph below), a soft signal activates if slow warnings occur

over 2 consecutive years, and were intended to identify the need for more intensive monitoring. In contrast, a hard signal activates if slow warnings occur for 3 of 4 consecutive years, or fast warnings occur for 2 out of 3 consecutive years (see below). In our example, hard signals are intended to stimulate management actions beyond additional monitoring that are aimed at stabilizing populations.

We applied these rules to annual rates of population change for sage-grouse as of 2016, whereby soft signals were activated across 17 leks and 7 neighborhood clusters, and hard signals were activated across 5 leks and 0 neighborhood clusters. Importantly, we estimated that sage-grouse populations across northeastern California and Nevada have declined at an average rate of 3.86 percent annually over the last 17 years. We then conducted a post hoc analysis to simulate how well activation of hard signals under the different rules (that is, the temporal threshold) and sequential increases in simulated management efficiency slowed rates of population decline. The results indicated that 2 of 3 consecutive years of fast warnings or 3 of 4 consecutive years of slow warnings achieved the greatest reduction in the long-term (that is, over a 17-year period) rate of population decline across the region-wide extent, and population stability could be brought about if all actions stabilized declining local populations.

Overall, this monitoring framework can facilitate effective adaptive management of an important indicator species for sagebrush ecosystems in near-real-time by incorporating adequate annual lek count data. Similar hierarchical approaches could be beneficial for other species occupying landscapes with heterogeneous disturbance and climatic regimes. Importantly, this framework is inherently adaptive in that the rules of the early warning system can be tailored to identify manageable patterns at the local lek and neighborhood scales. For example, higher resolution information could be achieved for targeting management actions by adding nested local-scales for sequential contrasting of population trends against each other and those at larger climate-driven scales. This approach could further guard against implementing management actions misaligned with the size of disturbances driving local population declines. The evaluation process can also be modified to identify other trends relevant to informing management actions, such as understanding when local populations are stable or increasing slightly, but nevertheless are underperforming compared to regional populations. The rules used in the framework could be modified further to identify when local populations are outperforming larger surrounding populations, which could help demonstrate where, and to what extent, restoration efforts are positively affecting local populations of sage-grouse. These examples highlight the flexibility of our framework to meet a variety of management needs.

Introduction

Population ecologists have long recognized the importance of aligning demographic processes to the appropriate spatiotemporal scale, where intrinsic and extrinsic factors drive those processes. Such an alignment is a fundamental requirement for understanding population dynamics (Levin, 1992). The contribution of environmental and anthropogenic factors responsible for regulating (density dependent) or limiting (density independent) population growth often differ when measured at varying extents; understanding these differences provides key information on the mechanisms underlying changes in population abundance (Bissonette, 1997, 2016; Fuhlendorf and others, 2002). Thus, spatial scales at which local populations operate must be defined and investigated if population growth and declines are to be truly understood. Similarly, populations can be limited or regulated at different temporal scales, such as short-term fluctuations in population abundance caused by demographic stochasticity (Morris and Doak, 2002), or long-term cyclic patterns driven by abiotic (for example, climatic variation influencing resource availability) and biotic effects (Ranta and others, 1995; Lindstrom and others, 1996).

When applying management actions to conserve wildlife populations, failure to account for scale-specific processes (spatial and temporal) can result in significant misinterpretation of observed patterns (Sadoul, 1997; Bissonette, 2016). If the environmental or anthropogenic threat responsible for population decline is misaligned with the subsequent implementation of management actions, such actions are likely to be unsuccessful (Epifanio, 2000; Cummings and other, 2006). Scale-specific, or hierarchical, monitoring strategies provide a powerful analytical approach that share and contrast information within and among spatial scales to identify where and when declines occur, and to investigate the corresponding local or regional drivers responsible for such population changes (for example, Wallace and others, 2010). When applied thoughtfully, such hierarchical strategies can identify not only populations that have become unstable, but also those populations that are not growing as fast (or are static) compared to neighboring populations that are increasing rapidly in response to widespread and favorable environmental conditions. However, implementation of hierarchical strategies has remained largely elusive for the management of many species, and particularly for those occupying expansive geographical ranges (Lindenmayer and Linkens, 2010). Hence, appropriate sampling designs and analytical frameworks are needed to separate processes between and among scales, and safeguard against spurious conclusions that might be drawn simply because of random variation in animal behavior or measurement errors. When inferences are derived regarding the rate of change in population numbers across multiple spatial scales, comparisons can be made between scales that allow for separation of scale-dependent factors affecting population growth. When populations are monitored over multiple years, techniques can be applied to account for uncertainty in the observation process arising from errors in detection or missing count data. This can ultimately allow prediction of the magnitude of population change within and among spatial scales with an associated level of uncertainty. Accurate detection of changes in the abundance of wildlife populations across spatial and temporal scales that may signal the need for management action also requires standardized methods for data collection and subsequent analyses (Pollock and others, 2002). Without standardization, it becomes increasingly difficult to separate estimated differences that could arise from true changes in the measured variable, versus those due to differences in methodologies used to measure and quantify the variable (Oakley and others, 2003).

The greater sage-grouse (*Centrocercus urophasianu*s; hereinafter sage-grouse) is a sagebrush-obligate species distributed throughout sagebrush ecosystems of Western North America. Sage-grouse are considered an indicator species for the health of sagebrush ecosystems, and an umbrella species for other sagebrush-obligate or semi-obligate species given their near complete dependence on this ecosystem for survival and reproduction (Rich and Altman, 2001; Rich and others, 2005; Rowland and others, 2006; Hanser and Knick, 2011). As of the turn of the twenty-first century, sage-grouse occupy roughly one-half of their former historical range (Schroeder and others, 2004; Miller and others, 2011), and have demonstrated marked population declines in many parts of their geographic range over the past 3–5 decades (Garton and others, 2011, 2015; Western Association of Fish and Wildlife Agencies, 2015).

The degradation and loss of sagebrush habitats have been attributed to a variety of factors, including conversion to agriculture and inappropriate livestock grazing (Anderson and Holte, 1981; Beck and Mitchell, 2000), invasion of exotic plants (Germino and others, 2016), encroachment of pinyon-juniper (Blackburn and Tueller, 1970; Miller and Rose, 1999; Davies and others, 2011), and energy development (Walker and others, 2007; Doherty and others, 2008, Green and others, 2016). Populations of sage-grouse in the Great Basin, and particularly those in northeastern California and Nevada that comprise more than 25 percent of the species range-wide distribution (Coates, Casazza, and others, 2016), are vulnerable to a novel disturbance cycle of wildfire and annual grass invasion that destroys sagebrush (Bradley, 2010; Chambers and others, 2016; Coates, Ricca, and others, 2016). Expanding populations of common ravens (*Corvus corax*), highly effective predators of sage-grouse nests in disturbed habitats, present additional and non-trivial threats (Coates and Delehanty, 2010). Accordingly, the species has undergone multiple evaluations for listing under the Endangered Species Act (U.S. Fish and Wildlife Service, 2015), the most recent of which stimulated unprecedented amendments to land management policy across millions of acres of federally managed land, particularly in the Great Basin (Bureau of Land Management, 2015). Rigorous monitoring strategies and analytical frameworks capable of detecting local and regional populations at risk of continuous and compounding decline, and eventual extirpation, are integral to the effectiveness of those plans.

Sage-grouse populations are linked spatially to leks (that is, traditional breeding grounds) that are surveyed annually across large spatial extents (Western Association of Fish and Wildlife Agencies, 2015). Hence, sage-grouse populations have an inherent hierarchical structure (Coates and others, 2014; Cross and others, 2016). Abundance of sage-grouse can fluctuate annually at the smallest and most local level of organization (that is, the lek) (Rich, 1985, Fedy and Doherty, 2011; Blomberg and others, 2012), which can be influenced by factors such as local surface disturbances altering habitat conditions and predator communities (for example, Gregg and Crawford, 2007; Coates and Delehanty, 2010). However, variation in climate and land cover can also explain population dynamics that cycle at broader spatial scales (Aldridge and Boyce, 2007; Aldridge and others, 2008; Fedy and Aldridge, 2011; Fedy and Doherty, 2011); yet, synchrony of growth patterns among populations can also decrease as inter-population distance increases (Lindstrom and others, 1996). These findings further indicate that management considerations include larger spatial extents when evaluating local population processes. For example, if the number of sage-grouse attending a lek declines by 50 percent over 1 year, knowing whether the decline was governed by local factors (for example, a surface disturbance from wildfire or anthropogenic development) compared to those occurring at larger spatial scales (for example, wide-spread drought) only becomes possible if trends at larger spatial scales are measured and contrasted to those populations exhibiting local declines. Furthermore, sage-grouse demographic performance can vary dramatically among populations and years (Schroeder, 1997; Moynahan and others, 2006). Hence, sage-grouse population dynamics are clearly subject to demographic and environmental factors that exert different pressure across spatial and temporal scales, underscoring the utility of hierarchical methods that identify differences in rates of annual population change within and among spatial and temporal scales.

Importantly, greater understanding of sage-grouse population dynamics for management application can be facilitated through a standardized monitoring and analysis framework that explicitly considers hierarchical relationships. This would allow for partitioning of local compared to regional effects driving population dynamics at a particular place in time without having to specifically model effects from a suite of all possible environmental covariates. This pattern-seeking framework could then be used to formulate covariate models that quantify mechanisms driving observed patterns. In the past, accounting for hierarchical relationships in population studies was largely intractable because of limitations in quantitative approaches. However, recent developments in analytical methods using Markov-chain Monte Carlo algorithms in a Bayesian statistical framework facilitate modeling of population trends within and among multiple ecological scales that also account for observation errors (for example, Clark, 2007; Kery and Schaub, 2012; Hobbs and Hooten, 2015). Spatially explicit counts of male sage-grouse attending breeding leks provide reliable data for analyses of population trends (Fedy and Aldridge, 2011; Dahlgren and others, 2016; Coates, Ricca, and others, 2016), and are well suited for Bayesian hierarchical modeling (Coates and others, 2014; McCaffery and Lukacs, 2016; Green and others, 2017; Monroe and others, 2017). Another obstacle to accounting for hierarchical relationships is organizing complex levels of population structure into biologically relevant and spatially nested scales for species occupying expansive geographical ranges, such as sage-grouse. However, sage-grouse populations are spatially organized around breeding leks (Coates and others, 2013). This property, coupled with accurate estimates of sage-grouse movements across large and remote areas owing to advances in GPS-telemetry, facilitates application of geostatistical analyses that identify nested-spatial aggregations of sage-grouse populations in relation to environmental features. In turn, these environmental features can either enhance or inhibit movements within and among populations, and allow for a modeling approach that describes the relative importance of the features to sage grouse at varying spatial scales. Resulting estimates of spatial organization further enable identification of populations that are subjected to more local-scale effects compared to those subjected to more regional-scale effects.

Study Objectives

We provide an example of a hierarchical population monitoring strategy for Nevada and northeastern California that can act as an early warning system for sage-grouse populations in need of immediate management action based on annual information on trends in abundance. The distribution of sage-grouse populations in Nevada and northeastern California covers greater than approximately 122,000 km^2 of sagebrush ecosystems (Coates, Casazza, and others, 2016), of which greater than 81 percent is managed by local, State, and Federal agencies. Because managers are responsible for such a large area yet often have limited resources, effective and efficient monitoring strategies need to identify areas where management action can be implemented readily and synchronized spatially to the specific scale where threats are occurring. However, identification of trends that signal population decline may need to be tempered using safeguards that protect against implementing action too soon owing to short-term population dynamics or errors in lek counts, or because local populations are simply tracking

population trends occurring at broader spatial scales driven by less-manageable stochastic factors (for example, population cycles driven largely by variation in climate). Our primary objectives were to:

1. Identify appropriate cluster scales that inform the hierarchical population monitoring framework. These scales will define the extent of population modeling and identify areas more likely to be influenced by local (that is, more manageable) compared to regional (that is, less manageable) factors.
2. Develop a multi-step evaluation process that quantifies sage-grouse population trends across multiple spatial scales on an annual basis and activates signals of management concern based on thresholds. First, two types of thresholds are established from retrospective simulations using 17 continuous years of annual lek count data that identify sage-grouse populations that: (1) depart negatively from stability (that is, destabilize); and (2) fail to track growth trends driven more by climate at large scales (that is, decouple). Importantly, destabilization and decoupling can occur at slow or fast rates. Second, warnings are activated only if both thresholds are crossed at a given rate. Lastly, signals are activated if warnings remain activated over a particular sequence of years, which can provide an indicator of management intensity that may be needed to slow and ultimately halt population declines at the corresponding scale.
3. Describe the status of sage-grouse populations in Nevada and northeastern California as of 2016 through the use of the evaluation process.

Study Area

The region of interest is characterized primarily by sagebrush habitats throughout Nevada and northeastern California comprising approximately 12.6 million ha. This extent approximated the total known sage-grouse distribution in Nevada and California. The flora in this region is typical of the Great Basin and consists of Wyoming big sagebrush (*Artemisia tridentata* ssp. *wyomingensis*), black sagebrush (*A. nova*), and low sagebrush (*A. arbuscula*) at elevations less than 2100 m, whereas mountain big sagebrush (*A. tridentata* ssp. *vaseyana*) occurs at higher elevations. Other shrubs common to the region include green rabbitbrush (*Chrysothamnus viscidiflorus*), rubber rabbitbrush (*Ericameria nauseosa*), snowberry (*Symphoricarpos* ssp.), western serviceberry (*Amelanchier alnifolia*), and antelope bitterbrush (*Purshia tridentata*). Trees commonly occurring in sagebrush habitat in the Great Basin include single-leaf pinyon (*Pinus monophylla*) along with Utah juniper (*Juniperus osteosperma*) and western juniper (*J. occidentalis*). Climate in the region is characteristic of high-elevation desert found in the Great Basin, with hot and dry summers and cold and snowy winters (Coates, Casazza, and others, 2016).

Methods

Terminology and General Conceptual Model

Throughout our monitoring framework example, we will use a variety of terms that refer to specific components of the analytical workflow. To help prevent confusion in terminology and meaning, we provide a key for commonly used terms in table 1. Of particular importance is our use of the term ‘population,’ which refers to a population within a specific spatial extent (that is, sage-grouse within a defined geographic boundary). For example, population could refer to all sage-grouse associated with a lek, or all sage-grouse associated with a cluster of several leks, in which case genetic exchange through immigration and emigration will occur. However, as population boundaries become larger such exchanges between other populations will be greatly reduced (and negligible at the largest spatial extents).

Table 1. Definitions for commonly used terms in the example early warning system.

Term	Definition
Population	An aggregation of sage-grouse occurring within a specified spatial extent.
Spatial extent	Geographic area over which a population is defined or spatial information is summarized.
Spatial scale	The unit of measure that describes quantitatively the spatial extent. Typically scale includes two components, grain and extent, where grain is the highest unit of measures at which a variable of interest is assessed.
Lek scale	The smallest scale of population organization in our example, measured as the geographic coordinates of traditional breeding locations (or leks) with associated annual counts of male sage-grouse attendance.
Cluster scale	Spatially nested and aggregations of leks, delineated as measureable polygons, used to define spatial extents for modeling sage-grouse demographic processes, which are delineated in rank order. Hence, increasing cluster scale refers to increasing spatial extents comprising all lower cluster extents (for example, a particular cluster at scale 5 includes multiple polygons of clustered leks belonging to scale 4, which in turn contains multiple polygons of clustered leks belonging to scale 3, etc.).
Neighborhood cluster	Refers specifically to cluster scale 2 in this example (see section, "Results"), whereby movements of grouse among clusters is relatively minimal and demography is governed largely by births and deaths rather than immigration and emigration. This cluster was ultimately chosen in our example to represent more local aggregations of leks and for contrasting population trends at smaller and more manageable scales against those occurring at larger and more climatically driven scales.
Climate cluster	Refers specifically to cluster scale 5 (see section, "Results"), whereby population dynamics are likely driven by larger scale variations, such as climate, that affect population cycles of sage-grouse. Drivers affecting clusters at this scale are likely less manageable by direct intervention.
Region	The full spatial extent encompassing all clusters, defined as the sage-grouse population range in Nevada and northeastern California (fig. 1).
Evaluation process	A series of sequential steps used to quantify sage-grouse population trends of management concern on an annual basis. These steps comprise thresholds, warnings, and signals. The evaluation process has safeguards against spurious and ephemeral spatial and temporal variation, and halts if criteria for any of the steps are not met.
Thresholds	Values determined through simulation analyses of 17 continuous years of annual sage-grouse lek count data that must be crossed to initiate step 1 of the evaluation process. There are two types of thresholds for determining populations in decline– destabilizing and decoupling. Destabilizing thresholds contrast the estimated rate of population change (λ) at the scale of interest relative to stability (that is, $\lambda = 1.00$). Decoupling thresholds contrast percent difference in λ at the smaller scale relative to the λ of a larger scale that it is nested within, which estimate how well population change at the smaller scale tracks population change at the larger scale. In our example, all smaller scale clusters (that is, lek and neighborhood cluster) are always contrasted against the climate cluster, and climate clusters are contrasted against the region. Importantly, thresholds for destabilizing and decoupling can be crossed at different rates of decline according to slow and fast criteria. Slow thresholds were intended to indicate slower rates of decline and decoupling, whereas fast thresholds were intended to indicate more precipitous rates of decline and decoupling that relate to high risk of extirpation.
Warning	Step 2 of the evaluation process, whereby a warning is activated if and only if both destabilizing and decoupling thresholds are crossed. Slow warnings activate if both slow thresholds are crossed. Fast warnings activate if both fast thresholds are crossed.
Signal	Step 3 of the evaluation process that requires a sequence of years with warnings (that is, a temporal rule or threshold) to activate a signal. These rules: (1) guard against transient population dynamics or imperfect surveys; and (2) evaluate the duration and magnitude of destabilization and decoupling. We propose two example signal types that may stimulate different management actions needed to stabilize or reverse estimated population declines: soft and hard. A soft signal activates if slow warnings occur over 2 consecutive years. A hard signal activates if slow warnings occur for 3 out of 4 consecutive years, or fast warnings occur for 2 out of 3 consecutive years.

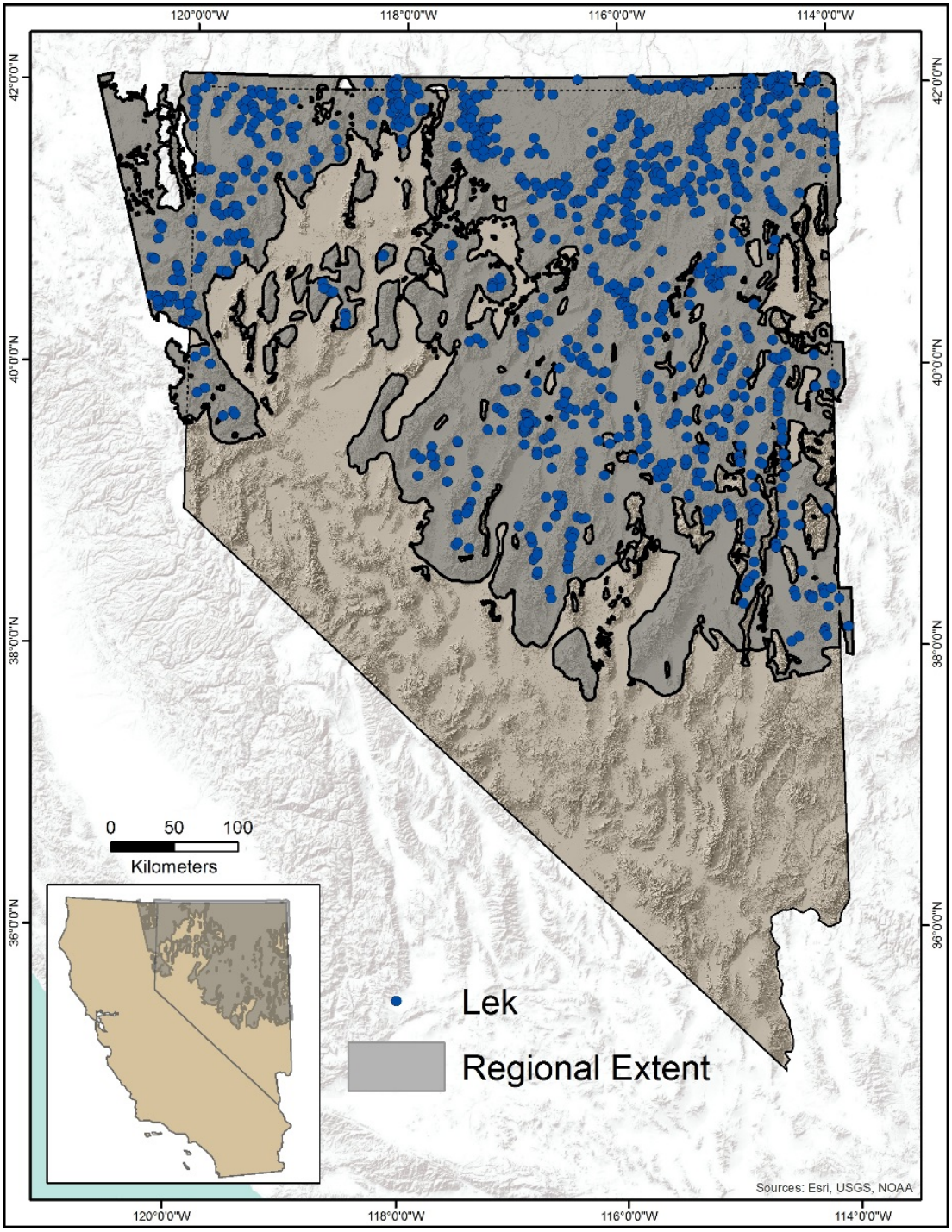

Figure 1. Map showing regional habitat extent and distribution of leks for greater sage-grouse (*Centrocercus urophasianus*) in Nevada and parts of northeastern California.

The flow-chart in figure 2 highlights the sequence of steps used in our example early warning system for declining sage-grouse populations. The approximate upper one-third of the chart represents data input and model output, which are then used to inform the three-step evaluation process represented in the lower two-thirds of the chart. We used lek count data to inform state-space models that estimated rate of population change (λ) at the lek scale. These estimates of λ were then weighted at the neighborhood cluster, climate cluster, and regional scales. We incorporated environmental covariates at each lek location to inform models used to delineate population cluster scales. Step 1 of the evaluation process involves assessing whether populations (at the lek, neighborhood cluster, and climate cluster scales) first cross spatial *thresholds* indicating: (1) destabilization (λ significantly less than 1.0) at a slow or fast rate; and (2) a decoupling of rates of population change at smaller scales compared to those occurring at larger scales at a slow or fast rate. In our example, lek and neighborhood cluster scales are evaluated for decoupling by contrasting trends against those occurring at the climate cluster scale. The larger cluster-scale is evaluated for decoupling by contrasting trends against those occurring across the regional scale. Crossing both thresholds provides initial evidence that factors driving possible declines are aligned with the appropriate scale, which then activates a slow or fast *warning* (step 2). In step 3, *signals* are activated if slow or fast warnings remain activated over a particular sequence of years (or temporal threshold) at a given spatial scale. Temporal thresholds for signal activation help guard against acting on spurious warnings in a single year that could result from variation in factors affecting lek attendance of males, and also help determine the duration and magnitude of destabilization and decoupling for the population of interest. Slow signals are intended to identify populations that are declining steadily over short time periods and perhaps require more monitoring and localized threat assessment, whereas fast signals are intended to identify populations at high risk of extirpation and perhaps requiring more active management owing to more prolonged slow population declines or precipitous declines over shorter time periods. The evaluation process stops if a rule at any point along the sequence of steps is not met. Throughout most of our report, we focus primarily on contrasting more local (that is, leks and neighborhood clusters) scales against the climate scale. However, these rules can be scaled up to evaluate how population trends at the climate scale track trends at the regional scale (that is, the full spatial extent of our study).

Figure 2. on next page. Conceptual flow-chart highlighting the sequence of steps used in an example hierarchical monitoring strategy that can serve as an early warning system for declining sage-grouse populations. The approximate upper one-third of the flow chart represents data input and model output used to inform the three-step evaluation process represented in the lower two-thirds of the flow chart. Black-outlined boxes represent data sources, blue-filled ovals represent statistical models, and blue-filled rectangles represent spatial scales relevant to each stage of the evaluation process. Thin light-orange parallelograms represent thresholds (spatial or temporal), the thin dark-orange parallelogram indicates both spatial thresholds have been crossed to activate a warning, and the thin red parallelogram indicates that a temporal threshold of sufficient duration has been crossed to activate a signal. Signals can then suggest the need for more monitoring of populations declining slowly over a short time period (soft signal, light-red squares), or active management for populations declining slowly over longer time periods or precipitously over short time periods (hard signal, dark-red squares). The evaluation process stops if a rule at any point along the sequence is not met (indicated by black-outlined circles with 'stop'). In the case of signaling at the climate scale, management is more difficult to implement owing largely to less controllable factors. Hence no example actions are illustrated

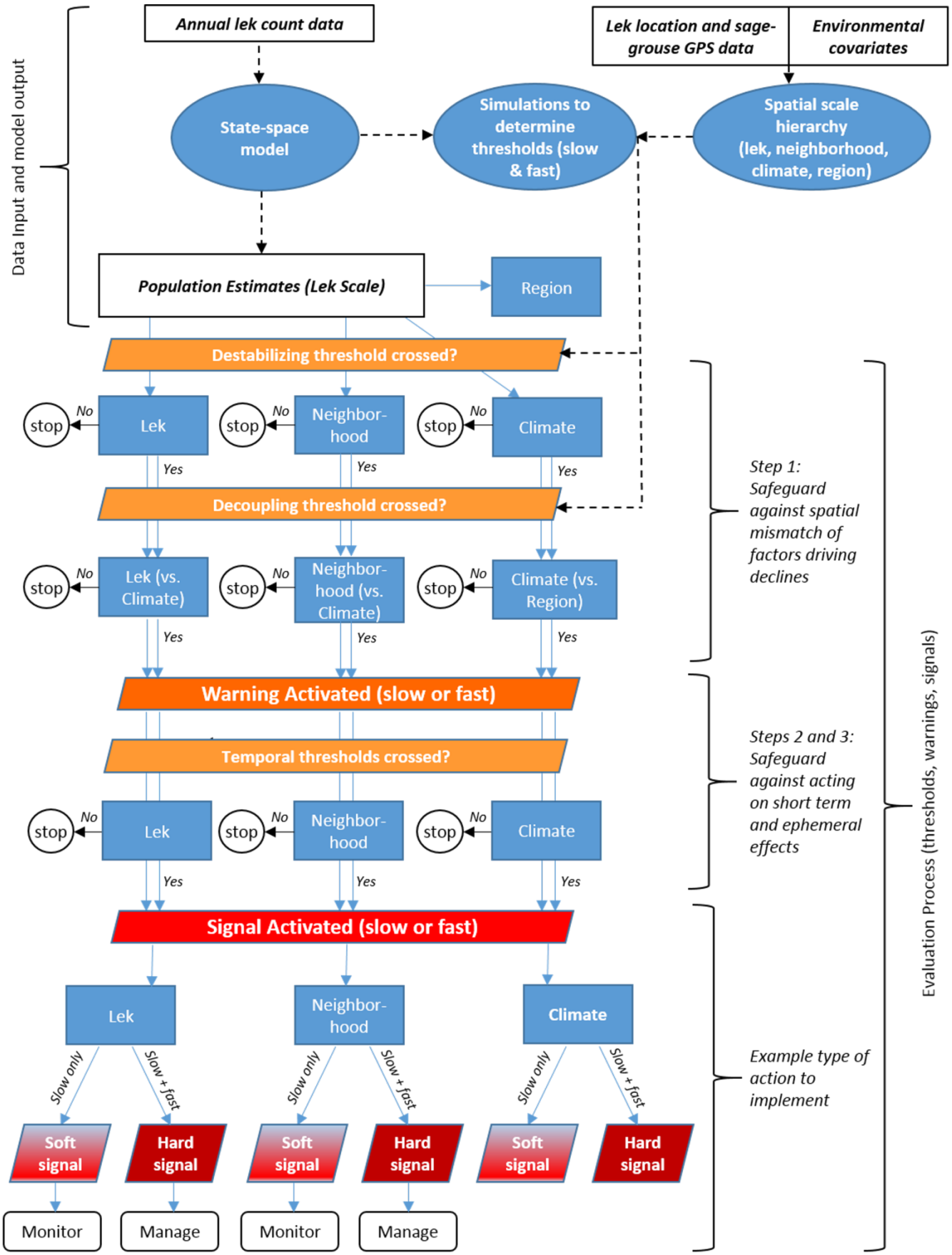
Annual lek count data
Lek location and sage-grouse GPS data
Environmental covariates
State-space model
Simulations to determine thresholds (slow & fast)
Spatial scale hierarchy (lek, neighborhood, climate, region)
Data Input and model output
Population Estimates (Lek Scale)
Region
Destabilizing threshold crossed?
stop
No
Lek
Neighbor-hood
Climate
Yes
Decoupling threshold crossed?
Lek (vs. Climate)
Neighbor-hood (vs. Climate)
Climate (vs. Region)
Warning Activated (slow or fast)
Temporal thresholds crossed?
Signal Activated (slow or fast)
Slow only
Slow + fast
Soft signal
Hard signal
Monitor
Manage
Step 1: Safeguard against spatial mismatch of factors driving declines
Steps 2 and 3: Safeguard against acting on short term and ephemeral effects
Example type of action to implement
Evaluation Process (thresholds, warnings, signals)

Defining Spatial Extent and Scale

Delineating Spatially Nested Clusters from Lek Locations

The first step in developing a hierarchical monitoring strategy involved the delineation of similar groups of lek locations for multiple, nested spatial scales, which we briefly describe here. We partitioned the Nevada and California sage-grouse distribution into nested hierarchical regions using lek locations, biologically relevant landscape characteristics of sage-grouse habitat, and lek habitat connectivity. We considered "Active" and "Pending" lek sites classified by the Nevada Department of Wildlife and California Department of Wildlife in our analysis. Leks categorized as active had two or more males observed within two or more of the last 5 years. Pending leks either lacked consistent breeding activity during the prior 3–5 surveys, or had not been surveyed during the past 5 years but were active previously. We buffered these leks using five spatial scales (500-m, 1,000-m, 1,500-m, 3,200-m, and 6,400-m), which represented patch and landscape scales commonly used by sage-grouse for habitat selection (Coates and others, 2013; Fedy and others, 2014). For each buffered lek, we summarized climate, vegetation, and terrain indices, and we used these in part to inform the clustering of the leks at each hierarchical scale. We constrained the geographic extent of the clusters to the current range of sage-grouse delineated by the U.S. Fish and Wildlife Service after modifying the extent to ensure inclusion of all known lek locations.

The landscape characteristics considered for the clustering of lek locations included bioclimatic variables from 30-year climate averages (O'Donnell and Ignizio, 2012), vegetation components (Xian and others, 2013), and terrain indices. We considered the following climate indices: precipitation totals, annual mean temperature, mean temperature during the wettest quarter, mean temperature during the warmest quarter, and the variation of monthly precipitation totals over the course of a year. The vegetation components, representing 2015 ground conditions, included shrub height and percent cover of sagebrush, herbaceous plants, bare ground, big sagebrush, and litter (Xian and others, 2013). We developed a hydrologically corrected 30-m Digital Elevation Model (DEM) from which we derived a Vector Ruggedness Measure (VRM; Sappington and others, 2007) and a Terrain Ruggedness Index (TRI; Riley and others, 1999). We developed the VRM for each buffered distance and summarized the TRI for each buffered distance. Like the climate and vegetation indices, we assigned the terrain indices to each lek location, respective of the evaluated scales.

To inform connectivity of lek locations, we assumed leks with a least-cost path to adjacent leks were the most likely neighboring leks that sage-grouse will visit within a season. To capture connectivity of leks, we developed a Least Cost Minimum Spanning Tree (LC-MST) using ESRI ArcGIS Pro (Cost Connectivity Tool), lek locations, and the hydrologically corrected DEM. We also incorporated the restriction of sage-grouse movements by identifying inter-lek movements and barriers to movements. We quantified the inter-lek movements in Nevada using a dataset of 230 sage-grouse marked with Global Positioning System (GPS) collars (Coates, Casazza, and others, 2016). We restricted that dataset to those birds (n=53) that demonstrated greater than or equal to ($\geq$) 1 inter-lek movement during the breeding season (March through May 2012–16). Each bird was assigned to a home lek based on capture site and if a bird moved within 400 m of a different lek (ESRI, 2011, Near tool,), we considered this as an inter-lek movement. We calculated the 95th percentile of all designated inter-lek movement distances and we rounded the mean (14.9 km, Standard Error = 0.451) to the nearest whole number to inform the connectivity between leks.

We defined barriers to sage-grouse movements by considering large topographic features and anthropogenic disturbances, which Knick and others (2013) incorporated in their ecological minimums evaluation. Using non-breeding season locations from 274 GPS collared birds within Nevada (2012–16), we constructed movement paths occurring within less than or equal to (≤) 2-day intervals. We inverted the statewide Nevada habitat suitability index (HSI; Coates, Casazza, and others, 2016) to represent resistance and then extracted raster values of the ecological minimums resistance surface and the HSI resistance surface along the constructed paths. We divided the disagreement between these results by the number of points used to create all movement paths. This proportion represented the time that the two surfaces disagreed on restrictions to movement. We then used the resistance value optimizing agreement (95th percentile) to set the threshold of the ecological minimums product, resulting in a barriers dataset. We modified the dataset when lek locations occurred within barriers and we removed small barriers that resulted from the inclusion of data with varying spatial scales of the ecological minimums.

We divided the LC-MST into three categories where each category informed a different hierarchical scale when clustering the leks. To create the first LC-MST category (hereinafter referred to as LC-MST 1), we enforced inter-lek movement distances of 15 km by deleting paths between leks longer than 15 km and paths between leks intersecting barriers. Because of the differing spatial scales of the ecological-minimums dataset relative to the data used in this analysis, we did not modify the LC-MST when its paths touched edges of large barriers. We then lessened the restriction of movement distances by allowing birds to move greater than 15 km, but they could not cross barriers (added paths >15 km back to the LC-MST; hereinafter referred to as LC-MST 2). The third LC-MST product (hereinafter referred to as LC-MST 3) did not enforce the inter-lek movement maximum distance threshold or barriers. We used the LC-MST 1, LC-MST 2, and LC-MST 3 to develop the finest scaled clusters, moderately scaled clusters, and coarsest-scaled clusters, respectively.

To create hierarchical scales of small and fine-scaled polygons (more representative of local and closed populations of sage-grouse) within increasingly larger and coarser scaled clusters (more representative of similar climatic and vegetation conditions influencing large metapopulations of sage-grouse), we used a clustering algorithm known as Spatial 'K'luster Analysis by Tree Edge Removal (SKATER; AssunÇão and others, 2006). We imported our three LC-MSTs into Program R (R Core Team, 2016) using the shp2graph library (Lu, 2014). We used the 'skater' function in the spdep library (Bivand and others, 2013; Bivand and Prias, 2015) for all clustering. Cluster scales 1–2 (fine scale) relied on the LC-MST 1, cluster scales 3–4 (moderate scale) relied on the LC-MST 2, and cluster scales ≥5 relied on the LC-MST 3 (coarse scale). When we created cluster scales 1, 3, and 5, we included all covariates (referred to as 'full' stage), but when we created cluster scales 2, 4, and ≥6, we considered the covariates identified from the previous cluster scales results (referred to as 'interim' stage).

We considered all univariate and multivariate cases during the full stage clustering of leks and we evaluated two spatial weighting methods of the covariate space (Euclidean and Mahalanobis distance). When we created the interim cluster scales, the covariates did not change, but we permitted the spatial weight to change. Each time we transitioned to a new cluster scale, we calculated the median of the raw covariates assigned to the leks within each cluster, and we constrained the SKATER algorithm to group a larger incremental number of leks. Because SKATER only supports connected graphs, we clustered and treated each subgraph independently. We used an agglomerative clustering approach where we started at the finest-scale clusters and we applied SKATER at each tier, thereby aggregating leks at each cluster scale. We identified the top cluster model of each cluster scale and subgraph using the Akaike's Information Criterion corrected for small sample sizes (AIC_c; Burnham and Anderson, 2002). After clustering the leks, we used ESRI's Desktop (ESRI, 2011) Thiessen Polygon tool to create polygons of the leks assigned to a cluster. The aforementioned methodology

produced a total of seven spatial extents (or "cluster scales"), which formed the basis of our hierarchical monitoring strategy. We selected a subset of these spatial extents using empirical data available from radio-marked sage-grouse so that the most biologically relevant scales were used in the monitoring strategy.

Selecting Cluster Scales for the Evaluation Process

For our example, we objectively selected two nested cluster scales (that is, 'neighborhood' and 'climate', in addition to the individual lek) to define sage-grouse populations for the evaluation process. We chose two cluster scales to simplify the analysis and facilitate a framework more amenable to management decisions and actions. In choosing the smallest scale of clustering, our goal was to represent a population level of organization (where movements between clusters is minimized) amendable to informing management actions aimed at reducing or eliminating adverse effects of landscape-scale impacts to sage-grouse populations (for example, wildfire). In choosing the larger cluster scale, the goal was to represent broad-scale factors (for example, climate) that govern population trends and are therefore difficult to influence through management action. However, too large of a larger cluster scale would result in the dilution of climatic and vegetation effects (as determined from the clustering analysis) that influence specific metapopopulations, because these effects would essentially be averaged across too large of an area (such as the regional scale). This created a twofold objective to: (1) reduce movement among clusters and allow for the assumption that the demographic rates within the cluster were driven more by births and deaths rather than immigration and emigration; and (2) minimize the area that a single cluster encompasses to reduce the variability in the remaining covariates (that is, not migration) responsible for driving changes in the vital rates within that cluster and be tractable for effective management. Accordingly, we term the smaller scale cluster as the 'neighborhood cluster' and the larger scale cluster as the 'climate cluster'.

We selected the neighborhood and climate cluster from the pool of all quantified cluster scales ($n = 7$) using the following steps. First, we removed GPS locations collected from sage-grouse used in the previous analysis to allow an independent dataset for assessing cluster break-points. Second, we randomly sampled this dataset to collect one point per bird per day. Each bird was assigned a unique ID. Third, we duplicated the methods presented by Coates and others (2013) to construct kernel density estimates of the utilization distribution (UD) for each bird. This was accomplished by calculating the volume of each UD within each cluster across all cluster scales delineated (methods outlined in previous section). The volume of each UD within each cluster was then divided by the total volume of the UD, which provided the proportional volume of the UD. Fourth, we estimated the maximum proportional volume to represent the home cluster for each bird, and then calculated the proportion of time (based on volume) each bird spent outside of the home cluster. For example, if a bird spent the entire time inside the same cluster, then its home cluster volume would be 1.0, and its proportional volume outside the home cluster would be $1.0 – 1.0 = 0.0$ (that is, no time was spent outside the home cluster). In contrast, if a bird spent 90 percent of the time inside the same cluster, then its home cluster volume would be 0.9, and proportional volume outside the home cluster would be $1.0 – 0.9 = 0.1$ (that is, 10 percent of time was spent outside its home cluster). The average proportional volume outside the home cluster and associated standard errors were calculated for all birds for each of the delineated cluster scales. Last, we selected the biologically relevant neighborhood cluster scale based on differences between the mean UD for each scale to minimize movement between clusters and appropriate spatial extents that are most amenable to resource managers. The climate-cluster scale was chosen based on the largest scale that exhibited clear separation from the neighborhood-cluster scale and did not differ significantly from the next largest cluster scale.

Evaluation Process

Modeling Population Change

We used a time series of lek data available for sage-grouse monitored across Nevada and California from 2003 to 2016 to estimate annual changes in abundance by applying state-space models fit in a Bayesian statistical framework (Kery and Schaub, 2012). Lek count data underwent several quality control checks by the Western Association of Fish and Wildlife Agencies (WAFWA) before they were compiled for use in our models (Coates, Ricca, and others, 2016). In addition to the WAFWA quality control checks, we developed a set of criteria that had to be met for leks to be included in the dataset analyzed. For every year and every monitored lek, we used the maximum number of males per lek recorded. A lek had to be counted a minimum of 5 times over the 17-year study period, and each lek had to be monitored for at least 1 out of the last 5 years to be included in our dataset. We marked missing data in the compiled data files for leks that met the last criteria but included some missing years (that is, a missing year received a "NA" in our data file), and years with missing data did not enter the likelihood of the state-space model. For every lek meeting these criteria, we added a value of one to the reported count. This was necessary to avoid division by zero, which yields an undefined calculation of λ. Lek counts formed the basis of population data at each spatial extent. At the smallest cluster scale (the individual lek), the annual rate of population change was estimated. At the cluster and regional scales, we took the posterior parameter estimates of λ (natural-log transformed) and calculated a weighted average (based on lek-level abundance) from every lek nested within a given boundary.

We used Bayesian state-space models to estimate N (that is, annual population abundance) and λ from the lek count data (Kery and Schaub, 2012; Coates and others, 2014; Green and others, 2017). These models assume constant or random variability in detection, which we confirmed prior to this analysis using a dataset of repeated double-blind ground counts, and aerial infrared surveys of artificial 'pseudo leks' (that is, tethered live pheasants spaced in lek-like configurations) with known abundance. When detection probability is less than 1.0 (that is, imperfect detection) but relatively constant across years, state-space models provide an unbiased index of population size and estimates of λ that represent trends in the sampled population. These models also provide a means of separating process variance (that is, environmental) from observation error (Kery and Schaub, 2012), which is done by partitioning each variance component using a hierarchical model, where:

$$N_{i,t+1} = N_{i,t} \times \lambda_{i,t} \quad (1)$$

$$\lambda_{i,t} \sim \text{Normal}(\bar{\lambda}_i, \sigma^2_{\lambda\ i})\text{T}(0,) \quad (2)$$

$$y_{i,t} \sim \text{Poisson}(N_{i,t}) \quad (3)$$

$$N_{i,1} = \text{Uniform}\ (0{,}60) \quad (4)$$

Here, the state process (equations 1 and 2) can be modeled while accounting for observation error (equation 3). Equation 3 maps the true state of the process onto the observed data ($y_{i,t}$), which in this case are individual maximum counts (y) at a given lek population (i) and year (t). Note that our use of "population" here refers specifically to an individual lek population. The errors in the counts were modeled using a Poisson distribution with a mean equal to the variance. Use of a Poisson error structure, as specified in equation 3, assumes that observation error increases as the "true" number of birds present on the lek increases, which was a reasonable assumption for counts of sage-grouse at leks. We assigned vague priors to the initial (t=1) population size of each lek (equation 4).

The state-space model produced a posterior distribution of the estimated parameters (that is, N and λ) for each population and year of the time series. The posterior is a probability distribution containing samples from the Markov chain Monte Carlo (MCMC) sampler which is used to produce statistics (for example, median and credible intervals) for a given parameter. These posterior distributions formed the basis of our inference for identifying thresholds for populations that destabilized and decoupled from a higher scale. Lambda (λ) for each site and year was distributed normally about the mean population-level λ. Sigma (σ^2) was given a uniform prior using the dunif function set at (0,10) in program JAGS (Plummer and others, 2015) run through the R interface. Site and year λ values were truncated using the T(lower, upper) function in JAGS, and was set as T(0,). Models were run in program JAGS using three chains of 15,000 iterations each following a burn-in period of 5,000 iterations. Chains were thinned by a factor of three. Model convergence was assessed using the R-*hat* statistic (Gelman and others, 2004). We did not find a lack of convergence among any of the parameters monitored (R-*hat* < 1.1).

These posterior distributions of λ estimates through time and across individual leks, neighborhood clusters, and climate clusters form the foundation of the early warning system and evaluation process. This system signals when populations may be in need of management intervention. Equally important, this system can be modified to provide a quantitative and defensible way to evaluate when past conservation actions have positively affected sage-grouse populations.

Determining Thresholds

We conducted a simulation analysis to estimate: (1) destabilizing thresholds designed to identify significant rates of population decline at a particular nested scale; and (2) decoupling thresholds designed to identify rates of population decline at smaller scales that decouple significantly from rates of population change at a larger spatial scale. Leks and the neighborhood cluster scale were contrasted for decoupling against the climate cluster scale, and the climate cluster scale contrasted for decoupling against the regional scale. The simulation retrospectively analyzed 17 continuous years of annual lek count data (2000–2016) to estimate relative probabilities of crossing different slow and fast thresholds on population stability. Crossing a slow destabilizing and decoupling threshold would indicate that the population was more likely to contribute towards probability of decline rather than probability of stabilization at the respective larger scale, whereas crossing a fast threshold would indicate that the population was more likely to contribute towards probability of extirpation rather than probability of decline at the respective larger scale. The steps used to estimate slow and fast destabilizing and decoupling thresholds are outlined as follows.

Slow Destabilizing Thresholds

1. We first used state-space models that account for process and observation variance to derive posterior parameter estimates (PPE) of λ for each lek every year. We converted estimates to intrinsic rate of change (r) using a logarithmic transformation. We then calculated r at neighborhood cluster and climate cluster scales by averaging the median lek estimate of r weighted by the observed number of sage-grouse on each lek. The purpose of weighting was to allow contribution of each lek to the larger scale as a linear proportion of its lek size, largely because we were focused on estimating λ from total abundance at larger spatial scales. We then exponentiated the weighted average to convert back to annual λ.

2. The next step was to identify a threshold of annual λ that contributed to population declines at each spatial scale. At the lek-, neighborhood-, and climate-cluster scales, we iteratively evaluated adjustments of λ from 0.02 to 1.00 by incremental unit increases of 0.02. Per iteration, λ was adjusted to 1.00 (stable) for all lek and year combinations with resulting median λ values that were less than the incremental value (fig. 3). The purpose of this step was to simulate neutralization of the most offending leks to those that were least offending in a systematic iterative process. For each increment, the lek and neighborhood cluster λ values (converted to r) were averaged (weighted) across each climate cluster. Similarly, the climate cluster λ values (converted to r) for each increment were averaged across the regional extent. This step simulated evaluation of how neutralizing all λ values at a particular increment at a lower scale resulted in overall population stability at the respective greater scale (fig. 3).
3. An increment that resulted in an average climate cluster (for leks and neighborhood clusters) or regional (for climate clusters) λ value equal to or greater than 1.00 (that is, stable or increasing), following an increment in which the λ value was less than 1.00 (that is, decreasing), was termed the separation point (fig. 3). This evaluation revealed those leks, neighborhood clusters, or climate clusters with λ values less than or equal to the separation point that contributed more to instability than stability (hereinafter, destabilizing units); whereas leks, neighborhood clusters, or climate clusters with λ values greater than the separation point contributed more to stability than instability (hereinafter, stabilizing units).
4. Distributions of λ values for destabilizing and stabilizing units were plotted against each other for leks, neighborhood clusters, and climate clusters. The intersection of these curves indicated the threshold for slow destabilization (fig. 4).
5. At predetermined ranges of λ values, we bracketed the estimated threshold by ± 0.05 (leks and neighborhood clusters = 0.85, 0.86, 0.87, 0.88, 0.89, 0.90, 0.91, 0.92, 0.93, 0.94, 0.95; climate clusters = 0.89, 0.90, 0.91, 0.92, 0.93, 0.94, 0.95, 0.96, 0.97, 0.98, 0.99). We then calculated the absolute value for the difference between probability densities ($\left|\Delta PD\right|$) of destabilizing and stabilizing units for leks, neighborhood clusters, and climate clusters.
6. At each predetermined location, the minimum $\left|\Delta PD\right|$ was divided by the $\left|\Delta PD\right|$ to derive a relative probability for the destabilized threshold value (fig. 5). A steep curve with a clear break in its peaks would indicate a high degree of certainty in the defined thresholds, whereas a flat peak would indicate a low degree of certainty in the thresholds.

Slow Decoupling Thresholds

1. Estimating slow decoupling thresholds involved two parts. The first part required estimation of individual population units at a smaller spatial scale (within lek, neighborhood, or climate clusters) that were responsible for contributing to slow destabilization rather than stabilization relative to their respective larger scale (described in section, "Slow Destabilizing Thresholds"). The second part required building a distribution to determine proportional changes (or deviation) in λ in the destabilizing population units at the smaller scale relative to the median λ of their respective larger scale (again, leks and neighborhood clusters against climate clusters; climate clusters against the entire region). This distribution allows identification of the decoupling threshold.

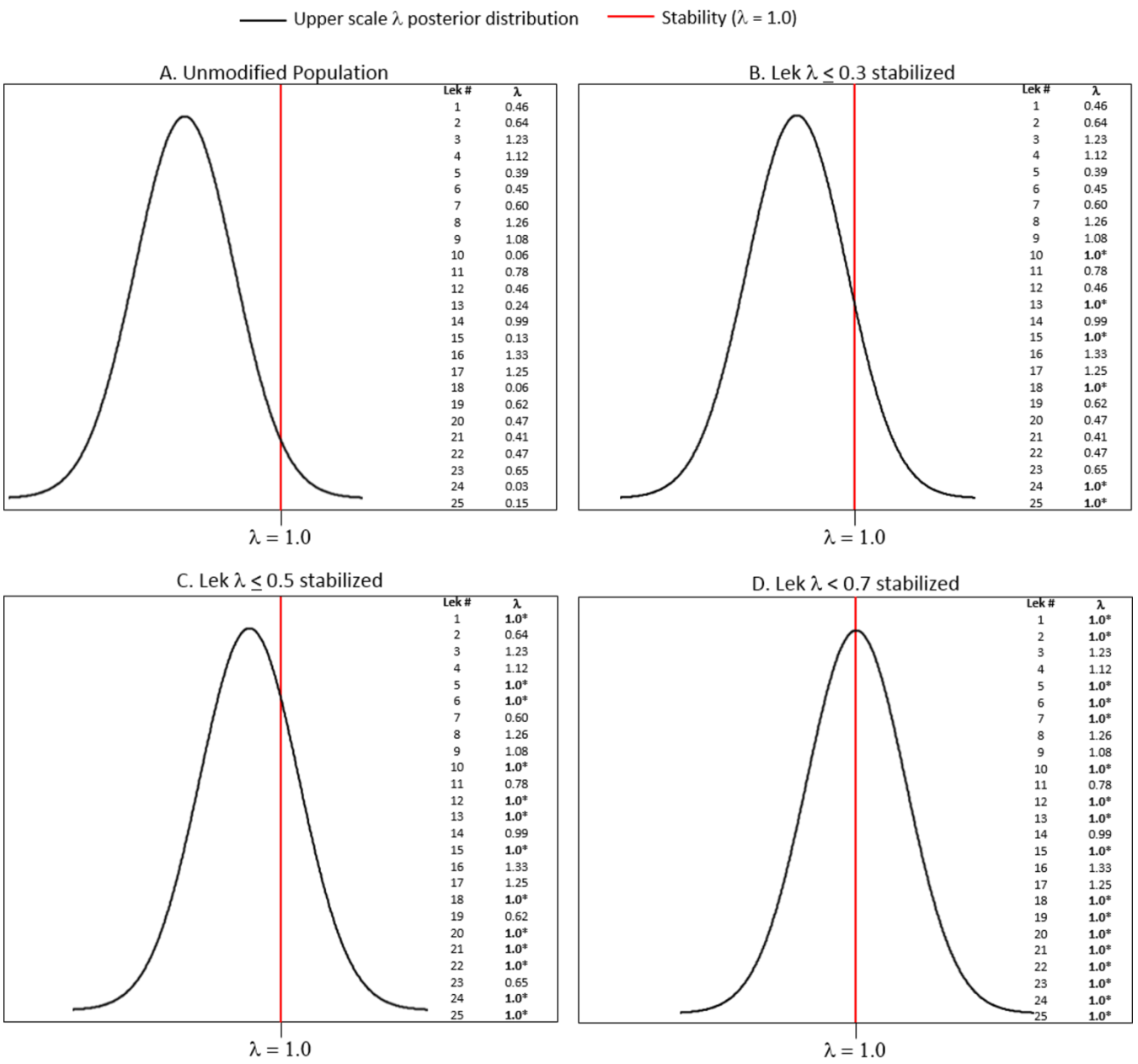

Lek #	A. λ	B. λ	C. λ	D. λ
1	0.46	0.46	**1.0***	**1.0***
2	0.64	0.64	0.64	**1.0***
3	1.23	1.23	1.23	1.23
4	1.12	1.12	1.12	1.12
5	0.39	0.39	**1.0***	**1.0***
6	0.45	0.45	**1.0***	**1.0***
7	0.60	0.60	0.60	**1.0***
8	1.26	1.26	1.26	1.26
9	1.08	1.08	1.08	1.08
10	0.06	**1.0***	**1.0***	**1.0***
11	0.78	0.78	0.78	0.78
12	0.46	0.46	**1.0***	**1.0***
13	0.24	**1.0***	**1.0***	**1.0***
14	0.99	0.99	0.99	0.99
15	0.13	**1.0***	**1.0***	**1.0***
16	1.33	1.33	1.33	1.33
17	1.25	1.25	1.25	1.25
18	0.06	**1.0***	**1.0***	**1.0***
19	0.62	0.62	0.62	**1.0***
20	0.47	0.47	**1.0***	**1.0***
21	0.41	0.41	**1.0***	**1.0***
22	0.47	0.47	**1.0***	**1.0***
23	0.65	0.65	0.65	**1.0***
24	0.03	**1.0***	**1.0***	**1.0***
25	0.15	**1.0***	**1.0***	**1.0***

Figure 3. Conceptual graphs showing how declining annual rates of population change (λ less than 1.0) at a lower scale (in this case, leks) were incrementally set to 1.0 to bring about simulated stability of known declining leks at an upper scale (in this case, the climate scale). Panel *A* shows a hypothetical distribution at the upper scale and the λ values at the lek scale that inform the distribution (inset table of 25 leks and corresponding λ values to the right). Panel *B* illustrates the shift in the distribution when leks with λ less than or equal to 0.3 are set to 1.0 (highlighted in **bold*** in inset table), Panel *C* illustrates the shift in the distribution when leks with λ less than or equal to 0.5 are set to 1.0 (highlighted in **bold*** in inset table), and Panel *D* illustrates the shift in the distribution when leks with λ less than or equal to 0.7 are set to 1.0 (highlighted in bold* in inset table). In this case, λ = 0.7 is the separation point where the median of the modified distribution meets or exceeds 1.0, which formed the separation point. In practice, λ was incrementally stabilized at intervals of 0.02 until the separation point was reached.

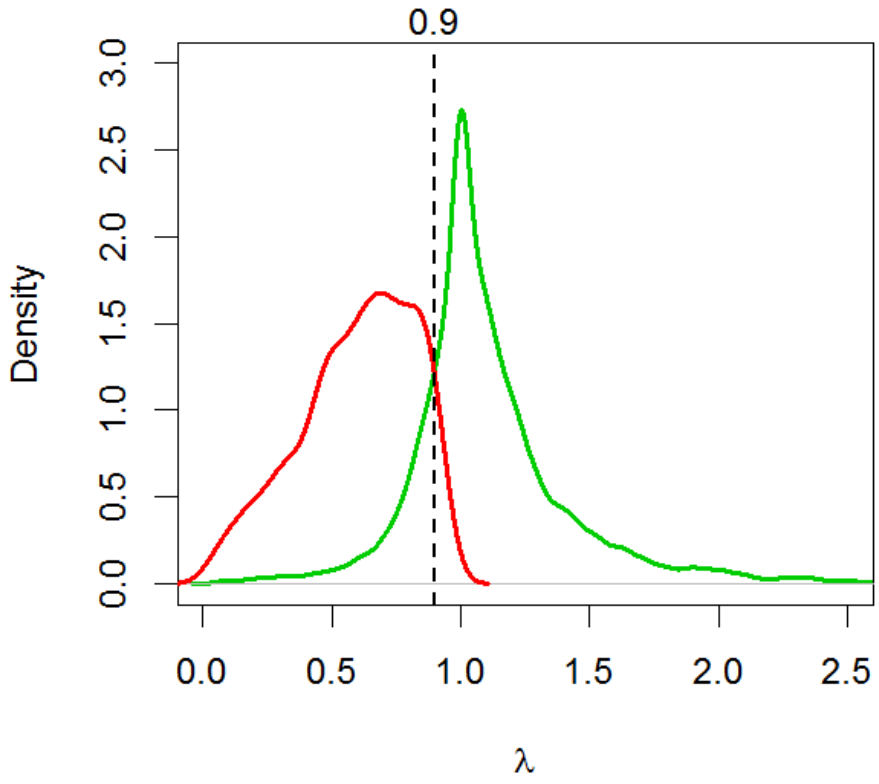

Figure 4. Graph showing distribution of annual rates of population change (λ's) for destabilizing lek units (red curve on the left side of the x-axis) and stabilizing lek units (green curve towards the right side of the x-axis). In a retrospective simulation analysis using 17 years of annual lek count data, destabilizing lek units had their λ values converted to 1.0 whereas λ values for stabilizing lek units remained unchanged (see fig. 3). The dashed vertical line represents the intersection between the two curves and indicates a slow destabilizing threshold of 0.90. The same process was conducted for neighborhood and climate clusters.

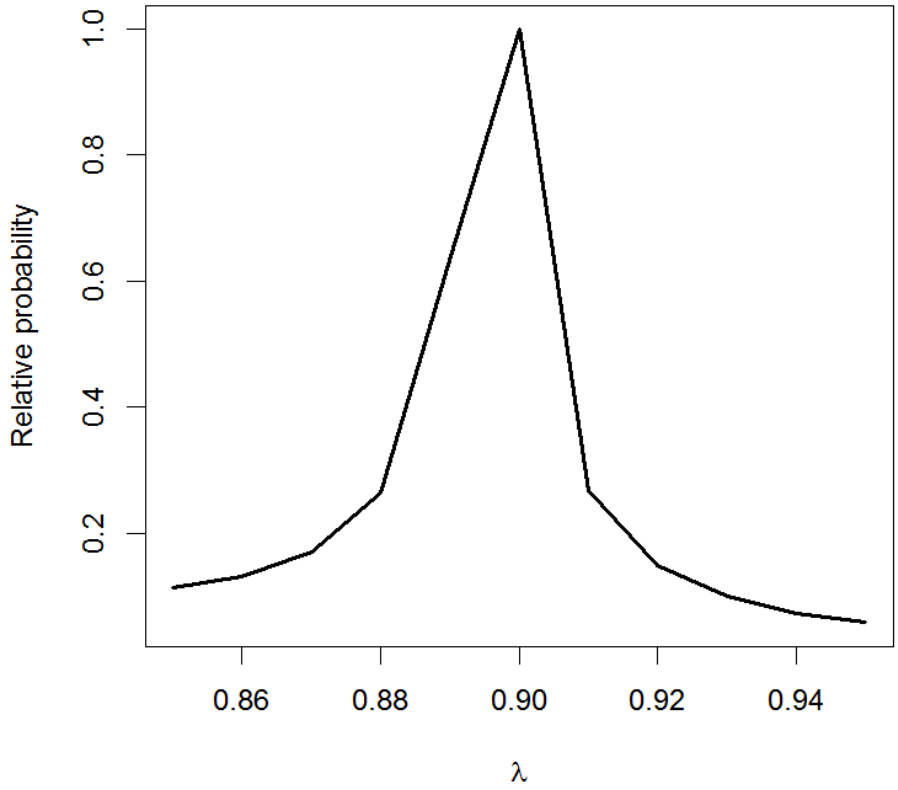

Figure. 5. Graph showing relative probability for the slow destabilizing threshold value (0.90), based on the difference between probability densities of stabilizing and destabilizing lek units. The steepness of the peak indicates a high level of certainty for the identified threshold. The same process was conducted for neighborhood and climate clusters.

2. To estimate the thresholds, we first calculated the median value of the PPE of λ for all destabilizing population units within lek-, neighborhood-, or climate-cluster scales. We then assigned that value to one of the 11 candidate threshold groups based on whether or not they were less than or equal to range of values (threshold ±0.05) described in step 5 in section, "Slow Destabilizing Thresholds" (that is, lek and neighborhood clusters group range = 0.85, 0.86, 0.87, 0.88, 0.89, 0.90, 0.91, 0.92, 0.93, 0.94, 0.95; climate cluster group range = 0.89, 0.90, 0.91, 0.92, 0.93, 0.94, 0.95, 0.96, 0.97, 0.98, 0.99).
3. Values of λ from the 11 threshold groups were sampled (with replacement) based on the relative probability of that threshold value (calculated in step 6 in section, "Slow Destabilizing Thresholds") (fig. 6).
4. Those 11 probability densities were then grouped into a single composite probability density (fig. 7).

5. Using this composite probability density, we calculated the change in the slope at 0.002 increments of λ within a range bracketed by the peak of the composite probability density, and 1.000. For example, if the peak occurred at 0.76, then changes in slope were calculated at 0.762, 0.764, 0.766, and so on, to 1.000. We chose 0.002 increments of λ to allow high resolution detection of changes in slope.
6. These changes in the slope were then divided by their maximum value (that is, the maximum change in slope) to derive a relative probability for the decoupling threshold value. The peak of this distribution represented the inflection point and indicated the threshold for slow decoupling (fig. 8). We selected the more protective inflection point that set the threshold at a higher level, rather than the median of the composite distribution (fig. 7), to guard against identifying decoupling at proportional changes more associated with rapid declines that are more difficult to stabilize.

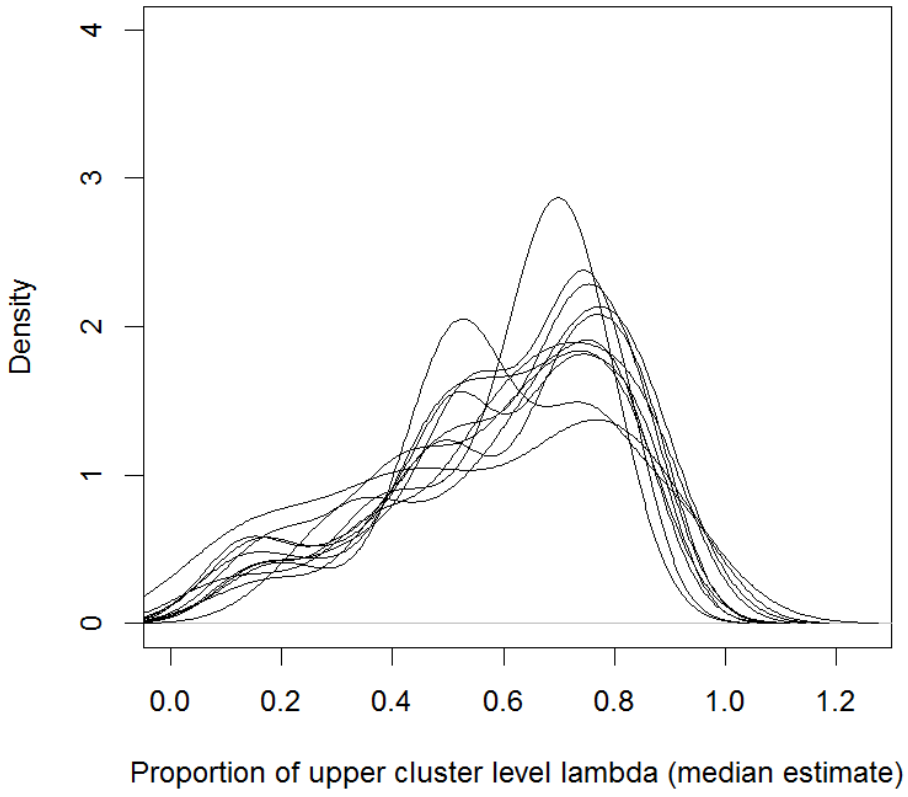

Figure 6. Graph showing probability distributions of λ for sage-grouse leks that were less than or equal to the destabilized threshold values (0.85–0.95).The proportion of samples used to inform each probability distribution was based on the relative probability for each destabilized threshold value. The same process was conducted for neighborhood and climate clusters.

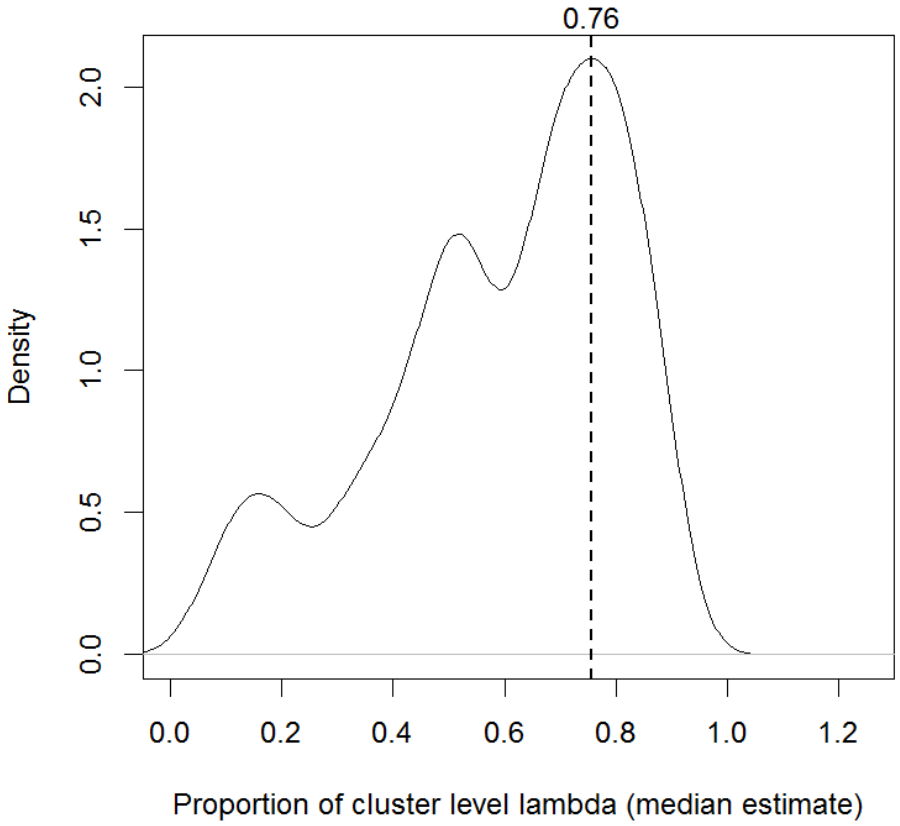

Figure 7. Graph showing composite probability distribution of λ values derived from figure 6 weighted by their relative probability. The vertical dashed line represents the maximum probability density for leks. The same process was conducted for neighborhood and climate clusters.

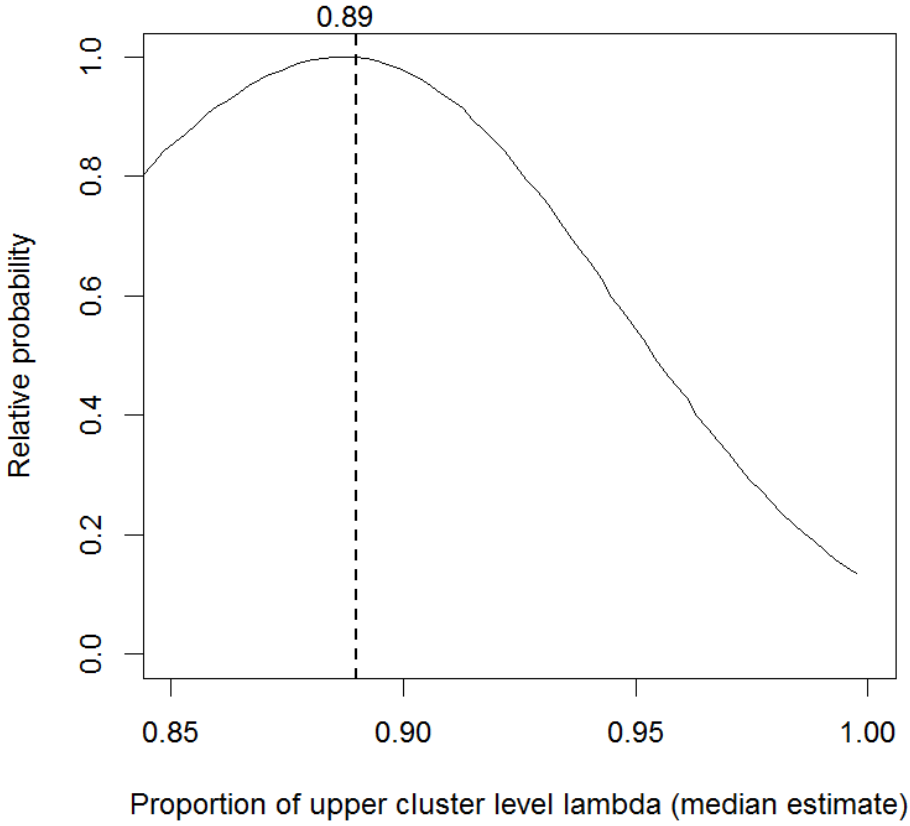

Figure 8. Graph showing relative probability for the slow decoupling threshold value, based on the change in slope of the composite probability distribution from figure 7. The example shown here illustrates the slow threshold for decoupling at the lek scale. The same process was conducted for neighborhood and climate clusters.

Fast Destabilizing and Decoupling Thresholds

Population units that contributed more to the probability of extirpation were used to identify thresholds for fast destabilizing and decoupling. Steps used were mostly identical to those described for slow destabilization and decoupling thresholds as previously described, with differences highlighted here.

1. We created a distribution of PPE derived λ values for "inactive leks" (that is, leks that went from an active status to an inactive status, and remained there, during the study). Using the same methods described in steps 1–6 of the "Slow Destabilizing Thresholds" section, we simulated separation points for leks with λ values more likely to contribute to extirpation compared to persistence probability. Here, destabilizing units (used for slow destabilization) were replaced with "extirpation-prone" units. We then intersected that distribution with the distribution for extant leks, identified the fast destabilization threshold using the point where the two curves intersected, and calculated the relative probability of that threshold.
2. We identified fast decoupling thresholds for leks with the same sequence of steps used for slow decoupling thresholds, but we used extirpation-prone rather destabilizing units.
3. Because no neighborhood or climate clusters were ever extirpated, it was impossible to calculate fast decoupling thresholds for these spatial scales using the same methods described for slow thresholds. Hence, for the neighborhood and climate scale, we adopted the same fast destabilizing and decoupling threshold values determined for leks.

Identifying Warnings for Declining Populations

After establishing the slow and fast destabilizing and decoupling thresholds, we contrasted the Bayesian state-space model output derived from the time series of lek count data to identify if thresholds at slow or fast rates at a particular scale had been crossed during a given year. We established a rule to guard against attributing population declines incorrectly to local rather than regional factors by requiring both types of thresholds to be crossed, whereby the posterior distribution of λ: (1) crossed the destabilization threshold; and (2) crossed the decoupling threshold (that is, the expected population growth rate at the next higher-order level). Depending on whether the thresholds were high or low, a slow or fast, respectively, warning is then activated and the population of interest proceeds along the evaluation process.

Figure 9 provides an illustration of the scenarios that would or would not activate a warning for a population of interest under a slow or fast threshold. In our example, these pertain to local populations at the individual lek or neighborhood-cluster scales relative to the climate scale, but can be extended to larger spatial scales (for example, the climate scale relative to the region). Patterns shown in figure 9*A*–*C* would not activate a warning because: the distribution of local population λ values is both stable ($\lambda \sim$ 1.0) and aligns (that is, is coupled) with regional population λ values (fig. 9*A*); the local population is stable but decoupled from the strongly growing regional population, which indicates that the local population is underperforming relative to growing populations at the regional scale (fig. 9*B*); or the local population has destabilized but has not decoupled because it is declining in relative synchrony with declines occurring at the regional scale, which could be indicative of an overall downward population trend across the region during climatically driven population cycles (fig. 9*C*). In contrast, patterns shown in figure 9*D* would activate a warning because the local population has destabilized, and is now decoupled from stable or growing patterns at the regional scale. In this case, potentially manageable disturbances may be associated with the beginning stages of population declines at the local scale that depart from broad-scale sage-grouse population trends likely driven by climatic variation.

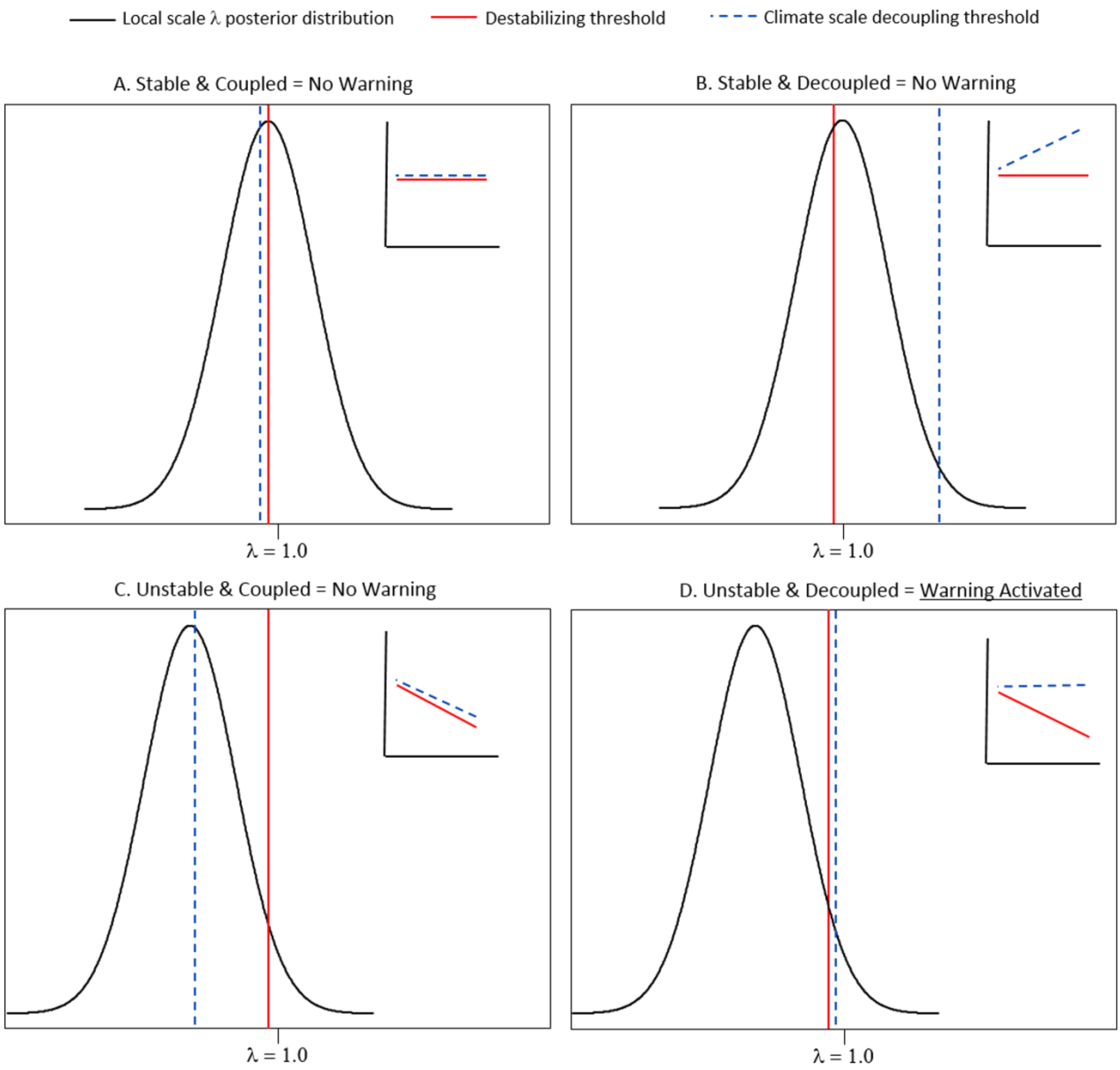

Figure 9. Graphs showing threshold crossings necessary to activate warnings within the evaluation process. In each panel, the bell curve represents the posterior distribution of λ values for population of interest at smaller spatial scales (for example, individual leks and neighborhood clusters), the solid red vertical line represents the destabilizing threshold where λ departs 'significantly' from 1.0, and the dashed blue line represents the decoupling threshold where λ at the smaller spatial scale relative to the median λ at the large spatial scale (for example, climate scale), whereby the proportional change in λ from the local to climate scale indicate high probability for decline or extirpation for the local population. The inset graphs represent destabilizing trends (solid red line) or decoupling thresholds (dashed blue line). Dashed blue lines that match red lines in the inset graphs indicate coupling, whereas those that do not match indicate decoupling. Panel *A* illustrates a scenario where the local population is both stable and matching trends at the higher scale. Panel *B* illustrates a scenario where the local population is stable but decoupled from trends at the higher scales, Panel *C* illustrates a scenario where the local population is declining but the pattern matches that of similar declines occurring at the higher scale (indicative of potential larger scale population cycles). Pattern *D* illustrates a scenario where the local population is both declining and decoupled from more stable patterns at the higher scale. Only Panel *D* warning activated because both thresholds have been crossed.

Importantly, our framework allows for evaluation of decoupling thresholds relative to any desired larger spatial scale that represents a biologically meaningful hierarchical level of organization, and patterns within lower spatial scales either can be contrasted against those at a single large-scale, or in a sequence of contrasting patterns, whereby smaller scales are compared to those at the next larger scale, and so-forth (for example, lek to neighborhood, neighborhood to climate). In our example, we chose to contrast all smaller spatial scales that represent lower levels of organization (populations and metapopulations) against those occurring at the larger climate cluster (see fig. 10). This reductionist approach of starting at the climate scale and then contrasting against successively nested local scales, allows for identification of how fine a scale is needed to identify where thresholds for decoupling have been crossed. This helps guard against implementing management actions that may be misaligned with the size of disturbances driving local population declines when signals are activated (see section, "Activating Signals for Declining Populations"). This approach can also be modified to yield higher resolution output for targeting potential management action by adding more nested spatial scales for sequentially contrasting population trends against those at larger climate-driven scales.

Activating Signals for Declining Populations

It is possible that spurious warnings in a single year could result from a variety of mechanisms unrelated to meaningful changes in population growth. These mechanisms include, but are not limited to: (1) short-term demographic stochasticity (for example, a short-term reduction in population performance possibly stemming from an ephemeral decrease in birth rates); (2) lek visitation rates (for example, a particular lek is subject to more variability among males attending that lek); or (3) measurement errors (for example, birds flushed from a lek before a count was taken, or incorrectly recording a zero count for a lek that was not actually counted). Criteria are also needed to evaluate how long destabilization and decoupling can occur before the population of interest is unlikely to recover despite management intervention. Therefore, the final step of the evaluation process incorporated temporal thresholds whereby a signal activates if slow or fast warnings remain activated over a particular sequence of years. These signals may then stimulate different management actions needed to stabilize or reverse estimated population declines.

Here, we propose two example signal types: *soft* and *hard*. To guard against potential problems caused by under-sampling, we set a rule whereby a lek required at least two counts over 5 years to activate a soft or hard signal. *Soft signals* activate if slow warnings occur over 2 consecutive years. We did not evaluate management effectiveness of soft signals because they are intended to identify populations that are steadily declining and perhaps require more monitoring and localized threat assessment before implementing any management action. In contrast, *hard signals* are intended to identify populations at high risk of extirpation where management actions could be implemented to ameliorate possible anthropogenic surface disturbance or land-cover change. Because extirpation risk could occur due to a steady and compounding decline (for instance, a series of slow warnings beyond 2 years), as well as under precipitous declining conditions (for instance, a sequence of fast warnings), we evaluated a series of combinations for activating signals under different durations of slow and fast warnings. Specifically, and for each scale, we activated signals over periods comprising 3 out of 4, 4 out of 4, and 4 out of 5 consecutive years of slow warnings, and combined each slow warning with fast warnings activated over 2 out of 2 or 2 out of 3 consecutive years. This design allowed for evaluation of six possible combinations of slow or fast warnings to reach a hard signal.

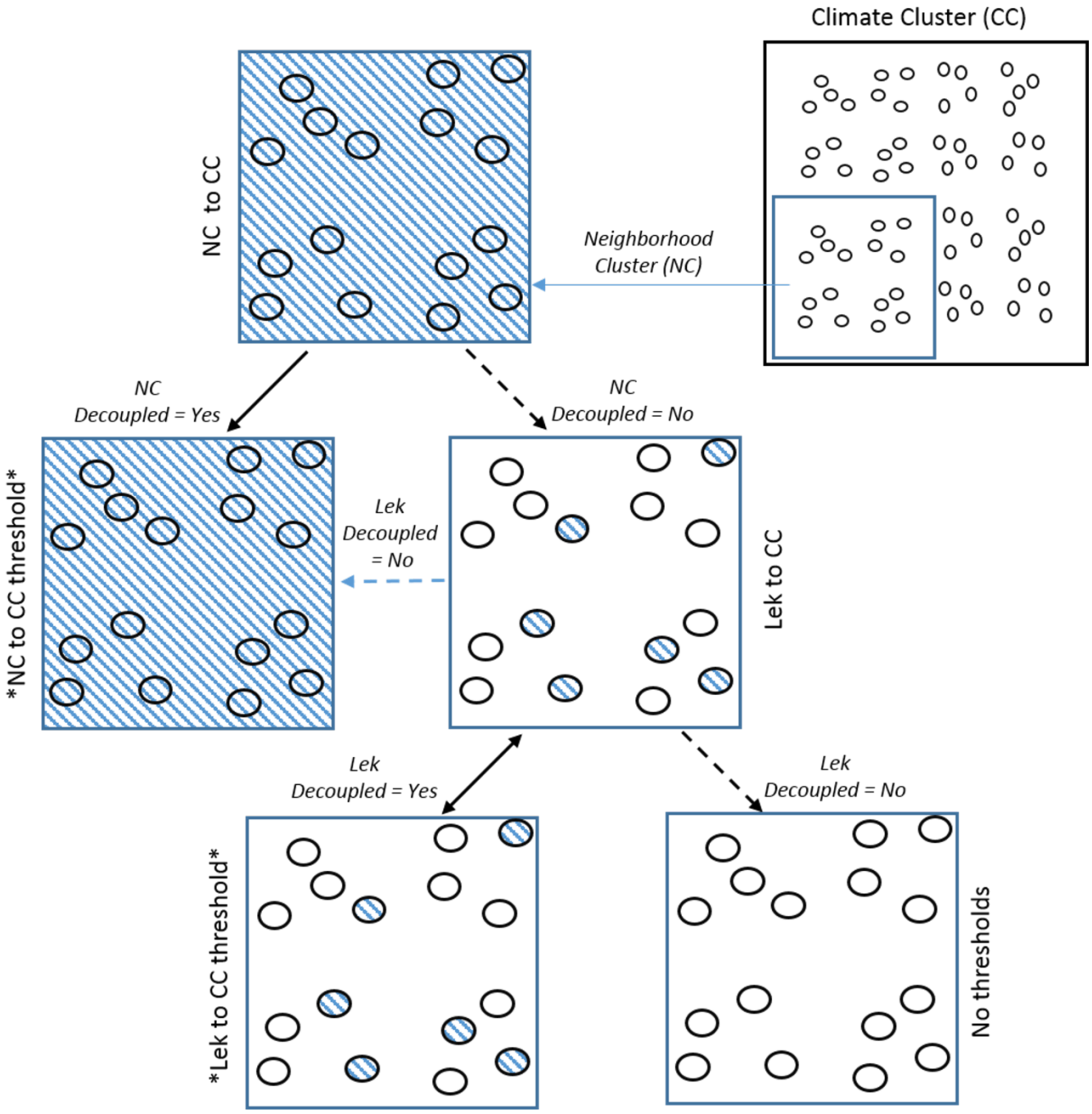

Figure 10. Conceptual model diagram showing how decoupling thresholds are contrasted from smaller spatial scales (that is, lek and neighborhood cluster) to a greater spatial scales (climate cluster) in a reductionist fashion. The black sided squares represents a climate cluster, blue-sided squares indicate neighborhood clusters, ovals within boxes represent leks, and blue hash-stripes indicate when thresholds for decoupling may have been crossed. In this example, decoupling at the neighborhood cluster is first evaluated. The neighborhood decouples significantly from its climate cluster when a threshold is crossed, and individual leks within are also not decoupled from the climate cluster. However, individual leks that decouple within neighborhoods can also be identified. If the decoupling threshold for the neighborhood is not crossed, the evaluation process continues to the lek scale relative to the climate cluster.

We conducted a simulation analysis to evaluate effectiveness of each combination of slow and fast warnings to identify the temporal threshold activating a hard signal that resulted in the greatest reduction in annual rates of population decline ($1 - \lambda$). For each combination, we simulated the effect of management action on improving λ by identifying all local populations (leks or neighborhood clusters) with a hard signal over the 17-year time series, and then adjusting the respective λ to 1.0 to neutralize the effect on the decline (hereinafter, *neutralized populations*). We ran these simulations assuming 100 percent management efficiency for all local populations with a hard signal (that is, all populations that had a hard signal over the course of the time series were neutralized), and then reduced management intensity in 10 percent increments (that is, neutralizing a random draw of 90 percent of populations that had a hard signal, then 80, 70 percent, etc.). We then calculated management efficiency as the change (or ratio) in neutralized λ compared to the original and unmodified λ. Thus, this simulation ultimately allowed for two types of comparisons: (1) differences in overall λ between varying temporal thresholds to reach a hard signal, and (2) differences in overall λ within each temporal threshold among varying management effectiveness. This simulation is necessary because a temporal threshold that is too long may result in implementing management action too late to rescue a population, whereas temporal thresholds that are too short remain prone to spurious warnings. Importantly, this simulation does not assume to identify the particular type of management action implemented and its subsequent effect on neutralizing specific mechanisms that are likely driving observed rates of decline. Rather, the term management is used in a strictly broad sense, and is implemented in our simulations with a generic approach.

Status of Sage-Grouse Populations as of 2016

We used the evaluation process for assessing thresholds, warnings, and signals to describe the status of sage-grouse populations in Nevada and northeastern California as of 2016. In particular, we described those populations at the lek and neighborhood cluster scales signaling the possible need for monitoring (soft signal) or active management (hard signal).

Results

Spatial Extents

A total of seven spatial extents were delineated based on the LC-MST approach and SKATER algorithm. These spatial extents consisted of seven distinct spatial cluster scales to represent hierarchical levels of population organization across Nevada and northeastern California. A total of 138 scale 1 clusters, 111 scale 2 clusters, 34 scale 3 clusters, 26 scale 4 clusters, 7 scale 5 clusters, 6 scale 6 clusters, and 5 scale 7 clusters were delineated. Delineated clusters were not always contiguous and clusters could be separated into fully disjoint polygons (for examples, see fig. 11).

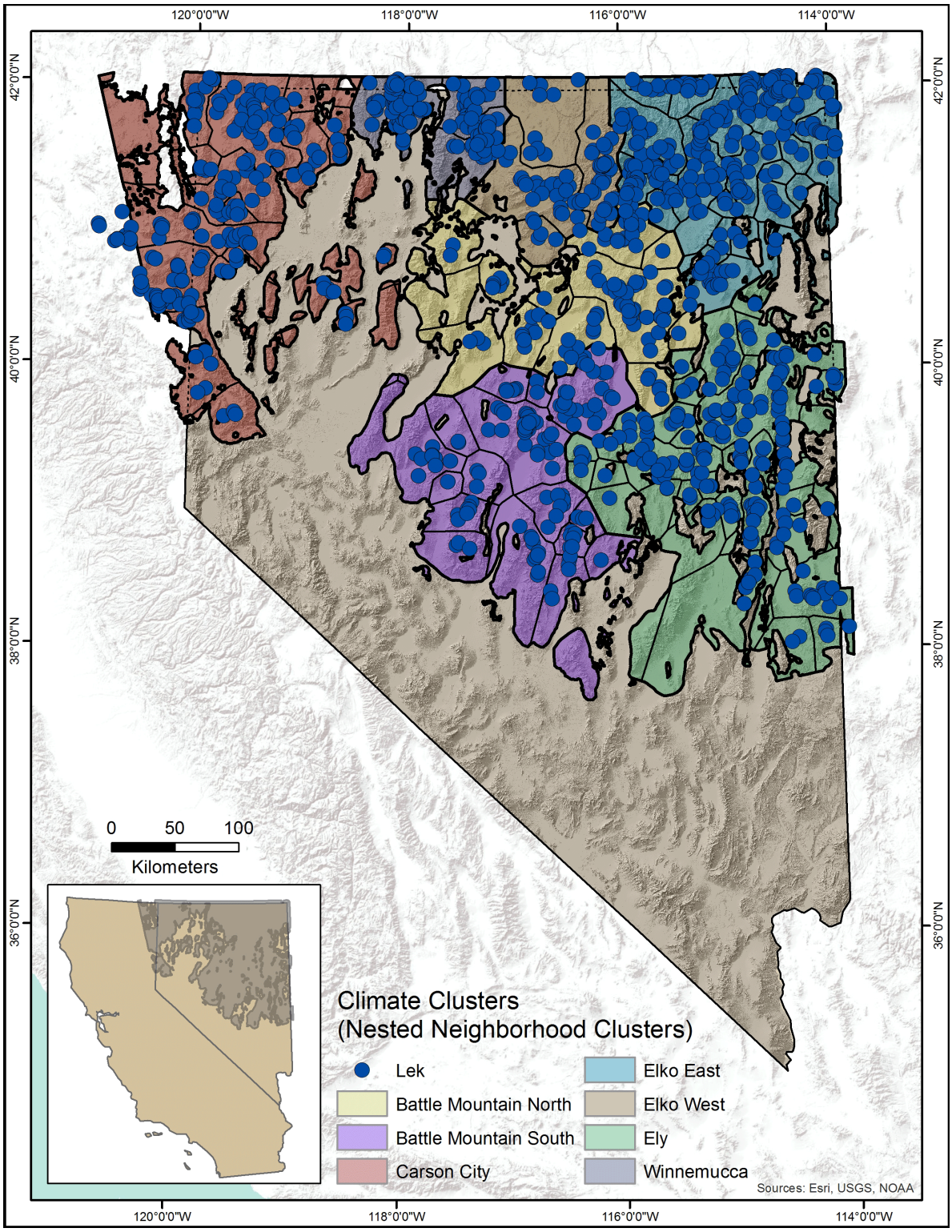

Figure 11. Map showing regional extent of greater sage-grouse (*Centrocercus urophasianus*) in Nevada and California. Lek locations (filled blue circles) that met criteria for inclusion in the analysis are shown along with their associated neighborhood clusters and climate clusters. Colored shaded areas represent climate clusters and delineated areas (black outlined polygons) within climate clusters represent neighborhood clusters.

Selection of Neighborhood and Climate Clusters

We calculated utilization distributions for the cluster scales delineated using GPS locations of individual sage-grouse to identify which scales were biologically relevant to hierarchical levels of population organization (for example, lek to population to metapopulation to region). Significant differences (based on non-overlapping confidence intervals) among cluster scales were found in the proportion of time sage-grouse spent outside their home cluster, which in general, was higher for scales 1 and 2 and diverged strongly from scales 5, 6, and 7 (fig. 12). We ultimately used cluster scale 2 to define the neighborhood cluster, and cluster scale 5 to define the climate cluster. We found evidence that cluster scale 3 aligned better with stronger population closure than cluster scale 2 to describe the neighborhood cluster scale. However, we used cluster scale 2 following feedback from a stakeholder setting, where it was expressed that cluster scale 2 offered better opportunities for more effective management actions (that is, management that could be implemented largely within a single management district) compared to cluster scale 3. In addition, all GPS-marked sage-grouse spent less than 6 percent of their time outside their home cluster scale 2, so we could assume that population dynamics at this scale were governed mostly by births and deaths within a closed biological unit small enough to allow local management. In contrast, metapopulation dynamics were likely well represented at cluster scale 5, where spatial extents were large enough to allow all GPS-marked sage-grouse to spend less than 2 percent of their time outside their cluster scale 5, and sage-grouse within these larger areas likely experienced similar climatic and habitat conditions. Individual lek and neighborhood clusters therefore represented local-scale populations, and their respective rates of populations change were contrasted against those occurring at the larger climate scale. Isolated neighborhood clusters without leks (n=4) were nested originally into a non-adjacent climate cluster. In these cases, we allowed these neighborhood clusters to adopt the identity of their respective adjoining climate cluster that contained leks. This post-hoc processing had no impact on the results of the signal analysis.Rates of population change at the climate scale were contrasted against those occurring at the full regional scale that encompassed all of Nevada and all but a few of the northeastern California populations of sage-grouse.

Thresholds

The simulation analysis produced a relative probability distribution of threshold values for slow and fast thresholds across all spatial scales of interest in our example. Slow destabilization thresholds had the highest relative probabilities at 0.90, 0.91, and 0.97, for leks, neighborhood clusters, and climate clusters, respectively. Fast destabilization thresholds had the highest relative probability at 0.55 for all spatial scales. Slow decoupling thresholds with highest relative probabilities for leks and neighborhood clusters relative to climate clusters were 0.89 and 0.92, respectively, and corresponding fast thresholds were 0.52 for both scales. Slow and fast decoupling thresholds with the highest relative probabilities for climate clusters relative to the region were 0.93 and 0.52, respectively.

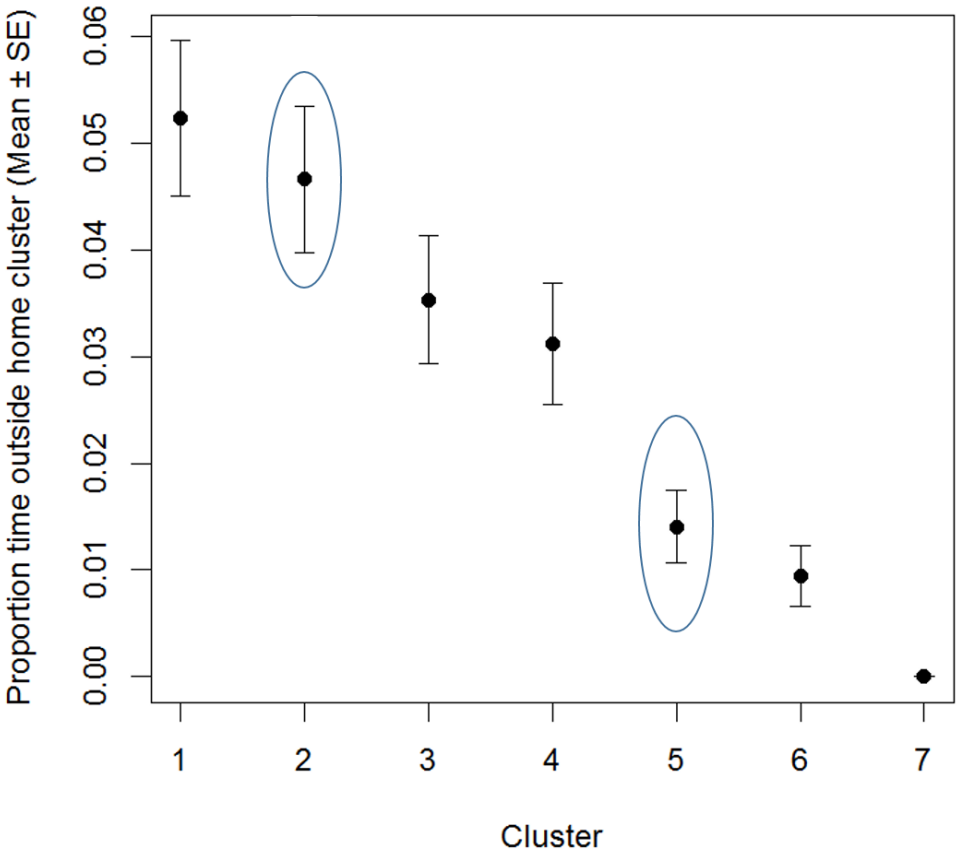

Figure 12. Graph showing comparisons of proportion of time GPS-marked greater sage-grouse (*Centrocercus urophasianus*) spent outside home clusters (that is, clusters outside of an area where birds were initially marked) across seven different cluster spatial extents. Mean proportions were calculated from the utilization distributions modeled for each bird. Cluster scales 2 (neighborhood cluster) and 5 (climate cluster), where selected to represent neighborhood and climate scales, respectively, in our example.

Applying Temporal Thresholds to Warnings, and Simulated Effectiveness of Signals

Soft signals (activated by 2 consecutive years of slow warnings) occurred on average for 6 and 7 percent of leks and neighborhood clusters, respectively, over the 17-year time series. When we applied our evaluation process over the 17-year time series under the different temporal threshold combinations for hard signals, 1 to 3 percent of leks and 1 to 2 percent of neighborhood clusters, respectively, had the requisite sequence of slow and fast warnings necessary to activate a hard signal (table 2). The greatest number of hard signals activated under 3 out of 4 consecutive years of slow warnings or 2 out of 3 consecutive years of fast warnings. In general, hard signals activated more frequently for leks with consistent survey effort, and for small and medium-sized leks than larger sized leks across all temporal threshold combinations. Hard signals also activated more frequently for clusters with consistent survey effort but with larger leks (table 2).

We did not evaluate management efficiency for soft signals because they only activated more intensive monitoring (but not active management) in our example. For hard signals, simulated management efficiency varied under the different temporal threshold combinations evaluated for activation (table 3). In comparing similar management efficiency across leks and clusters that activated hard signals, λ improved the most for leks and neighborhood cluster populations under the rule of 3 out of 4 consecutive years of slow warnings or 2 out of 3 consecutive years of fast warnings, and the pattern held across most levels of management intensity. Conversion of these ratios to values that reflected the percent simulated improvement on the reduction in the 17-year rate of annual population decline over the following 17 years ($1 - \lambda$) more clearly illustrated how this rule for hard signals consistently outperformed the other candidate rules (table 4). These improvements were nearly twice as high as those simulated under 4 consecutive or 4 out of 5 consecutive years of slow warnings combined with either 2 consecutive or 2 out of 3 consecutive years of fast warnings. They were also at least three-times as high as those simulated under the same sequence of fast warnings but with 4 consecutive years of slow warnings. Moreover, this rule was the only one to bring about simulated long-term stability when all management was assumed to be effective (that is, 100 percent), and cut the rate of decline by roughly one-half at 50 percent management intensity (table 4). Similar but slightly lower improvements were observed with the same sequence of slow warnings but allowing 2 consecutive years of fast warnings. Accordingly, we selected the 3 out of 4 consecutive years of slow warnings or 2 out of 3 consecutive years of fast warnings as the most protective temporal threshold for activating a hard signal for our example.

Status of Sage-Grouse as of 2016

When the entire evaluation process was applied to sage-grouse populations as of 2016, soft signals were activated across 17 leks (fig. 13). The majority of soft lek signals were located in the Ely climate cluster (9), followed by Elko East (4), Battle Mountain North (2) and Carson City (2). No leks were activated as soft signals within the Battle Mountain South, Winnemucca, and Elko West climate clusters. At the neighborhood cluster scale, soft signals activated at 7 clusters (fig. 14). The most soft signals activated in clusters in Ely (3), followed by Battle Mountain North (2), Elko East (1), and Carson City (1). No soft signals activated within climate clusters that were contrasted against the regional scale.

As of 2016, hard signals activated at 5 leks located within the Elko East (2), Battle Mountain North (1), Ely (1), and Battle Mountain South (1) climate clusters (fig. 15). Hard signals did not activate at any neighborhood clusters in 2016. No soft or hard signals activated at any climate clusters in 2016. When averaged annually over the last 17 years at the regional scale, λ was 0.961 (95% CI = 0.904–1.02). This corresponded to an average and long-term rate of annual decline of 3.86 percent. No hard signals activated within climate clusters that were contrasted against the regional scale.

In comparison to previous years, 2016 had relatively fewer leks and neighborhood clusters with activated hard signals (table 2). Under our selected temporal threshold (that is, 3 out of 4 consecutive years of activated slow warnings or 2 out of 3 consecutive years of activated fast warnings), all hard signals activated at either large- or medium-sized leks with consistent survey effort.

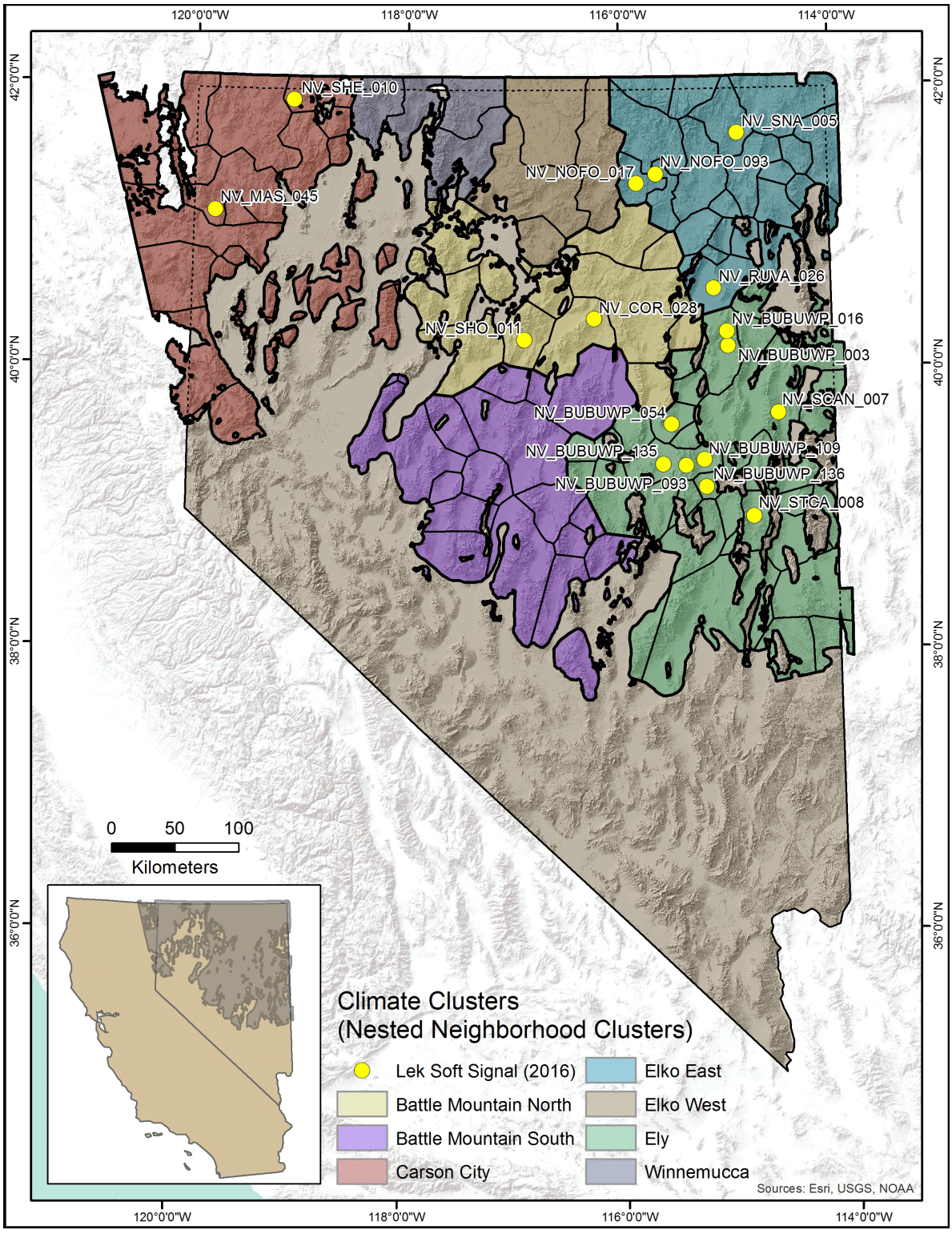

Figure 13. Map showing locations of greater sage-grouse (*Centrocercus urophasianus*) leks that met the criteria for a soft signal in 2016. Colored shaded areas represent climate clusters, and delineated areas (black outlined polygons) within climate clusters represent neighborhood clusters.

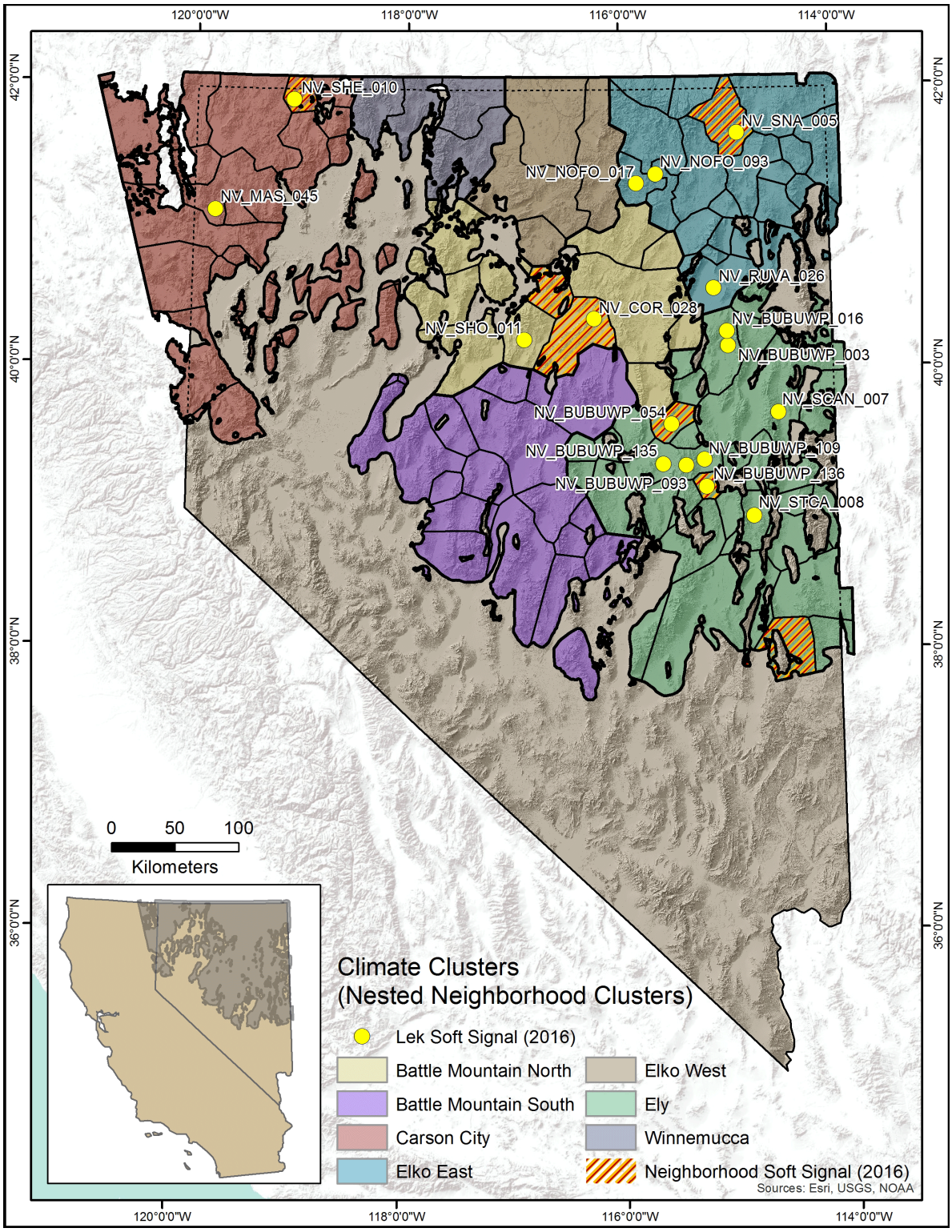

Figure 14. Map showing locations of greater sage-grouse (*Centrocercus urophasianus*) leks and neighborhood clusters that met the criteria for a soft signal in 2016. Colored shaded areas represent climate clusters and delineated areas (black outlined polygons) within climate clusters represent neighborhood clusters.

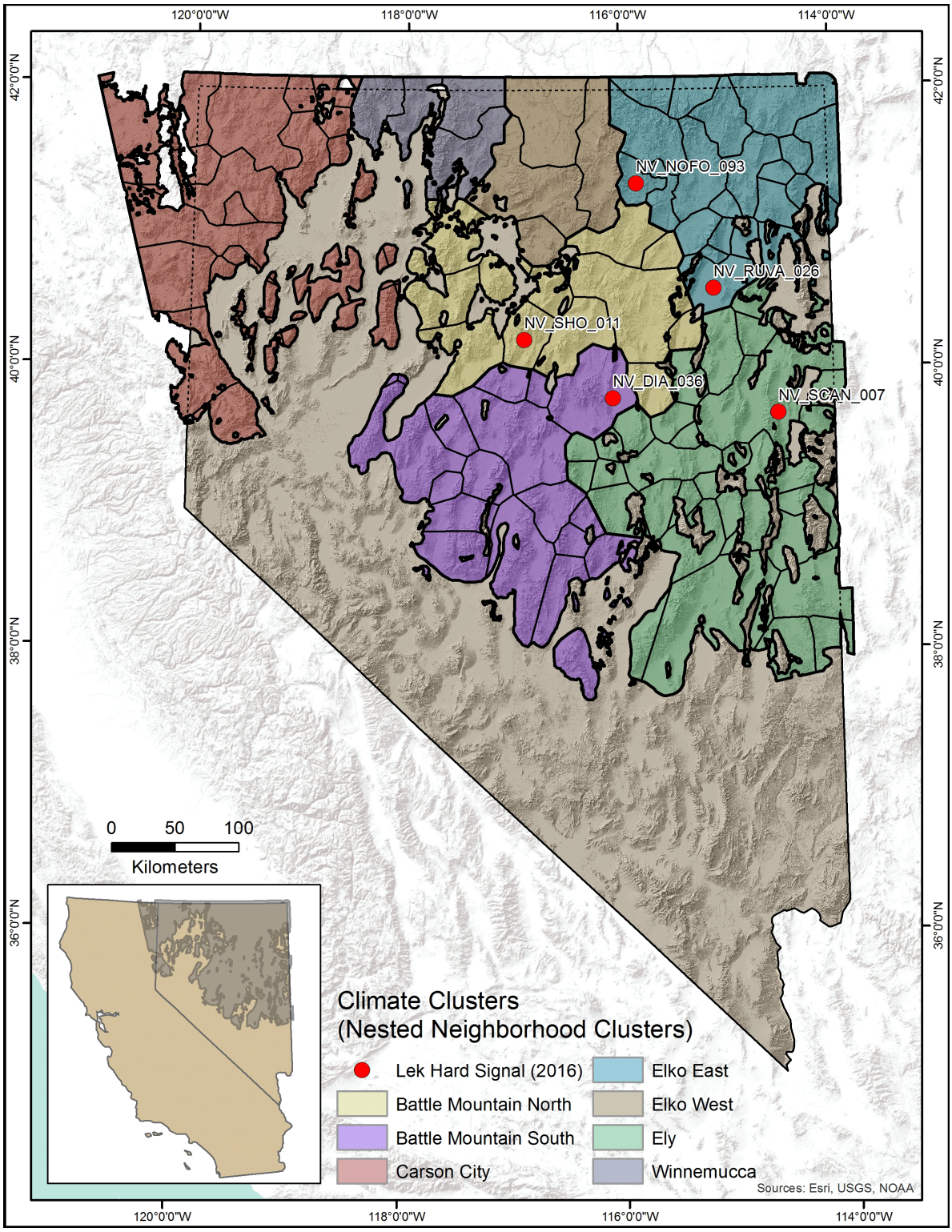

Figure 15. Map showing locations of greater sage-grouse (*Centrocercus urophasianus*) leks that met the criteria for a hard signal in 2016. Colored shaded areas represent climate clusters and delineated areas within climate clusters (black outlined polygons) represent neighborhood clusters.

Table 2. Descriptive statistics for declining sage-grouse (*Centrocercus urophasianus*) populations in Nevada and northeastern California that activated a hard signal under different combinations of slow and fast warnings across all years (2000–2016) and for 2016.

[Number of hard signals are also presented in relation to sample size (that is, number of lek counts conducted) and lek size (that is, average number of males on a lek over a 5-year period) categories that corresponded with a hard signal. Samples size categories that indicated the number of counts conducted over a 5-year period were: > 3 (greater than three lek counts), 3 (three lek counts), and 2 (two lek counts). Lek size categories were: Large (L) (greater than 29 male sage-grouse counted, Medium (M) (11–29 male sage-grouse counted), Small (S) (less than 11 male sage-grouse counted)]

Population	Slow warning (years)	Fast warning (years)	Hard signal - all years		Hard signals - 2016		Hard signal - all years						Hard signals - 2016					
							Sample size category			Lek size category			Sample size category			Lek size category		
			Average Proportion	Average Number	Proportion	Number	>3	3	2	L	M	S	>3	3	2	L	M	S
Lek	3 out of 4	2 consecutive	0.02	12.0	0.01	5.0	106	19	19	62	58	24	5	0	0	3	2	0
		2 out of 3	0.03	12.6	0.01	5.0	112	20	19	66	59	26	5	0	0	3	2	0
	4 consecutive	2 consecutive	0.01	4.7	0.01	5.0	33	16	77	20	22	14	3	2	0	2	3	0
		2 out of 3	0.01	5.4	0.01	5.0	44	18	7	25	24	16	3	2	0	2	3	0
	4 out of 5	2 consecutive	0.01	7.6	0.01	5.0	57	19	15	30	32	29	4	1	0	2	2	1
		2 out of 3	0.02	7.6	0.01	5.0	63	20	15	35	33	30	4	1	0	2	2	1
Neighborhood cluster	3 out of 4	2 consecutive	0.02	1.8	0	0.0	16	3	2	2	12	7	0	0	0	0	0	0
		2 out of 3	0.02	1.8	0	0.0	16	3	2	2	12	7	0	0	0	0	0	0
	4 consecutive	2 consecutive	0.01	0.8	0	0.0	6	2	1	0	6	3	0	0	0	0	0	0
		2 out of 3	0.01	0.8	0	0.0	6	2	1	0	6	3	0	0	0	0	0	0
	4 out of 5	2 consecutive	0.01	0.9	0.01	1.0	6	3	2	0	6	5	0	1	0	0	0	1
		2 out of 3	0.01	0.9	0.01	1.0	6	3	2	0	6	5	0	1	0	0	0	1

Table 3. Management efficiency scenarios for greater sage-grouse (*Centrocercus urophasianus*) populations in northeastern California and Nevada under different combinations of slow and fast warnings for activating hard signals from 2000 to 2016.

[For each combination, local populations that signaled were neutralized by setting the annual rate of population change (λ) = 1. Management efficiency is defined as the change in λ between the simulated neutralized populations and the original unmodified populations. Management intensity ranged from 100 to 10 percent (%) and varied by 10% intervals, where 100% indicated that management stabilized all populations (lek or cluster) that signal, 90% indicated that management stabilized 90% of populations that signaled, and so forth. Standard errors are in parentheses for management intensities less than 100%]

Local Population	Slow warning (years)	Fast warning (years)	Percent change in λ (neutralized: modified signals) with stated management efficiency				
			100%	90%	80%	70%	60%
lek	3 out of 4	2 consecutive	1.0206	1.0185 (0.0003)	1.0164 (0.0003)	1.0144 (0.0005)	1.0124 (0.0004)
		2 out of 3	1.0219	1.0196 (0.0003)	1.0175 (0.0004)	1.0154 (0.0005)	1.0131 (0.0005)
	4 consecutive	2 consecutive	1.0087	1.0078 (0.0002)	1.0070 (0.0002)	1.0060 (0.0003)	1.0052 (0.0003)
		2 out of 3	1.0102	1.0092 (0.0002)	1.0082 (0.0003)	1.0071 (0.0003)	1.0061 (0.0003)
	4 out of 5	2 consecutive	1.0135	1.0122 (0.0002)	1.0108 (0.0003)	1.0094 (0.0004)	1.0081 (0.0004)
		2 out of 3	1.0149	1.0133 (0.0003)	1.0119 (0.0003)	1.0104 (0.0005)	1.0089 (0.0004)
Neighborhood cluster	3 out of 4	2 consecutive	1.0192	1.0172 (0.0018)	1.0154 (0.0017)	1.0135 (0.0015)	1.0114 (0.0014)
		2 out of 3	1.0194	1.0175 (0.0019)	1.0155 (0.0017)	1.0136 (0.0016)	1.0116 (0.0014)
	4 consecutive	2 consecutive	1.0023	1.0021 (0.0001)	1.0018 (0.0002)	1.0016 (0.0002)	1.0014 (0.0002)
		2 out of 3	1.0025	1.0023 (0.0002)	1.0020 (0.0002)	1.0017 (0.0002)	1.0015 (0.0002)
	4 out of 5	2 consecutive	1.0090	1.0080 (0.0009)	1.0072 (0.0009)	1.0063 (0.0008)	1.0054 (0.0007)
		2 out of 3	1.0092	1.0082 (0.0010)	1.0074 (0.0009)	1.0064 (0.0008)	1.0056 (0.0007)

Local Population	Slow warning (years)	Fast warning (years)	Percent change in λ (neutralized: modified signals) with stated management efficiency				
			50%	40%	30%	20%	10%
lek	3 out of 4	2 consecutive	1.0102 (0.0005)	1.0081 (0.0005)	1.0062 (0.0005)	1.0040 (0.0004)	1.0020 (0.0003)
		2 out of 3	1.0109 (0.0005)	1.0086 (0.0005)	1.0065 (0.0004)	1.0043 (0.0004)	1.0022 (0.0003)
	4 consecutive	2 consecutive	1.0044 (0.0003)	1.0034 (0.0003)	1.0025 (0.0003)	1.0017 (0.0002)	1.0009 (0.0002)
		2 out of 3	1.0051 (0.0003)	1.0041 (0.0003)	1.0031 (0.0003)	1.0021 (0.0003)	1.0010 (0.0002)
	4 out of 5	2 consecutive	1.0067 (0.0004)	1.0054 (0.0004)	1.0040 (0.0004)	1.0027 (0.0003)	1.0013 (0.0003)
		2 out of 3	1.0074 (0.0004)	1.006 (0.0005)	1.0044 (0.0005)	1.0029 (0.0003)	1.0015 (0.0003)
Neighborhood cluster	3 out of 4	2 consecutive	1.0096 (0.0011)	1.0076 (0.0009)	1.0057 (0.0008)	1.0038 (0.0006)	1.0020 (0.0004)
		2 out of 3	1.0097 (0.0011)	1.0078 (0.0011)	1.0057 (0.0008)	1.0038 (0.0006)	1.0020 (0.0004)
	4 consecutive	2 consecutive	1.0012 (0.0002)	1.0009 (0.0002)	1.0007 (0.0001)	1.0005 (0.0001)	1.0002 (0.0001)
		2 out of 3	1.0012 (0.0002)	1.0010 (0.0001)	1.0007 (0.0002)	1.0005 (0.0001)	1.0002 (0.0001)
	4 out of 5	2 consecutive	1.0045 (0.0006)	1.0035 (0.0006)	1.0027 (0.0005)	1.0018 (0.0004)	1.0009 (0.0002)
		2 out of 3	1.0045 (0.0007)	1.0036 (0.0005)	1.0027 (0.0004)	1.0018 (0.0004)	1.0009 (0.0002)

Table 4. Effect of simulated management efficiency scenarios (described in table 3) on percent improvements on the annual rate of population decline and subsequent translations into simulated annual rate of population change across the region-wide extent of greater sage-grouse (*Centrocercus urophasianus*) populations in northeastern California and Nevada from 2000–16 under different combinations of slow and fast warnings for activating hard signals.

[Calculations used the region-wide average annual rate of population decline over 17 years of 3.86 percent as the baseline]

Slow warning (years)	Fast warning (years)	Percentage (%) of simulated improvement on the 17 year region-wide rate of annual population decline (1-λ) with stated management intensity (at decreasing intervals of 10%)									
		100%	**90%**	**80%**	**70%**	**60%**	**50%**	**40%**	**30%**	**20%**	**10%**
3 out of 4	2 consecutive	99.0%	88.9%	79.2%	69.5%	59.3%	49.3%	39.1%	29.6%	19.4%	10.0%
	2 out of 3	[1] **102.9%**	92.4%	82.2%	72.2%	61.5%	51.3%	40.8%	30.4%	20.2%	10.5%
4 consecutive	2 consecutive	27.4%	24.7%	21.9%	18.9%	16.4%	13.9%	10.7%	8.0%	5.5%	2.7%
	2 out of 3	31.8%	28.6%	25.4%	21.9%	18.9%	15.7%	12.7%	9.5%	6.5%	3.0%
4 out of 5	2 consecutive	56.0%	50.3%	44.8%	39.1%	33.6%	27.9%	22.2%	16.7%	11.2%	5.5%
	2 out of 3	60.0%	53.5%	48.1%	41.8%	36.1%	29.6%	23.9%	17.7%	11.7%	6.0%

[1] Value greater than 100% indicate simulated management actions brought about stability and increasing growth over the following 17 years.

Discussion

Summary of Overall Findings

We described a new framework for estimating annual sage-grouse trends across biologically linked and hierarchical population structures. This unique approach can now be applied to sage-grouse population management, and builds off recent advancements in Bayesian state-space population modeling (Coates and others, 2014; McCaffery and Lukacs, 2016; Green and others, 2017; Monroe and others, 2017) and likelihood-based hierarchical modeling (Monroe and others, 2016) for sage-grouse. Our example serves as a quantifiable and defendable early warning system for identifying populations that may be in need of habitat management actions to reverse population declines. This helps fulfill a prominent need for informing management of sage-grouse populations under recently approved land-use planning amendments (Bureau of Land Management, 2015).

In highly dynamic ecosystems that experience dramatic climatic shifts (such as cold deserts of the Great Basin), understanding the difference between when populations are responding naturally to weather related patterns compared to experiencing more localized- and habitat-based declines is a critical component of a monitoring system. Our monitoring system is unique in that we devised a novel way to reduce the noise in sage-grouse population dynamics caused by climatic fluctuations, ultimately increasing the speed and precision in our ability to detect populations in need of management intervention. This also can reduce the time and energy that managers spend responding to leks that are actually declining due to climate related (and less manageable) effects. Contrasting rates of population change at smaller spatial scales that represent local population levels of organization against those expected if a population was tracking similar trends occurring at larger spatial scales allows for such fluidity. Though not done in our example, further examination of soft or hard signals for more localized populations (leks or neighborhoods) that are contrasted against population trends at larger scales (likely driven by climate) can allow for post hoc evaluation of possible surface disturbances (for example, wildfire, grazing) impacting sage-grouse (Coates, Ricca, and others, 2016; Monroe and others, 2017). In addition, contrasting population rates of change at the climate cluster scale against those occurring across the entire region can help identify metapopulations in possible peril. Further research is planned to address these types of evaluations within a second phase of our population analyses.

Several spatial and temporal safeguards are built-in to this early warning system. A population must first cross a threshold leading to destabilization. However, local population declines highlighted by a destabilization threshold may be simply tracking larger-scale population cycles. In these instances, managers could incorrectly attribute declines to local factors that are not responsible. Therefore, we calculated a second threshold to account for the decoupling of the local trend with larger scales in the hierarchy. This spatial safeguard allows for only those populations most likely to be in decline for reasons other than mechanisms occurring at the larger scale to activate a warning, which then allows the evaluation process to proceed. We also designed a series of temporal thresholds to guard implementing management action on detected population declines that are likely an artifact of sage-grouse behavior or sampling error. For example, a warning might activate in a single year simply because few male sage-grouse visited a lek on the day it was surveyed because males were visiting other leks (Fremgen and others, 2017), or the lek was not surveyed but was recorded erroneously as a zero-count. Estimates of abundance derived by state-space model can help smooth these errors (however, see section, “Caveats”). Nevertheless, warnings could be activated falsely because of the shortcomings of the state-space model framework and (or) sampling methods, which is partly why we chose a multi-year system of warnings and signals. Our rule of 2 consecutive years of slow warnings to activate a soft signal is highly

protective, and prone to counting errors that would only need to repeat 2 years in a row. However, soft signals only indicate the need to monitor populations more closely in our example, and implementation of more intense monitoring of populations with falsely activated soft signals will likely result in subsequent soft-signal deactivation. However, additional monitoring may also identify leks that are truly in decline. In contrast, activation of hard-signals requires a longer sequence of slow decline (3 out of 4 consecutive years with slow warnings), or a shorter burst of precipitous declines (2 out of 3 consecutive years with fast warnings). Simulated management actions indicated these temporal thresholds were most protective of populations at high-risk of extirpation.

Our example framework also has applications beyond those described heretofore. For instance, our framework is simple in that it allows for identification of population trends in the absence of effects of spatially explicit environmental covariates. Although additive and multiplicative models are certainly capable of explaining more variation in a response than univariate models, they typically involve information-theoretic comparisons between several candidate models and subsequent averaging of effects, which can be computationally intensive and time-consuming in a Bayesian framework. In addition, the availability of spatially explicit and time-dependent covariate data across broad extents (for example, PRISM climate data [Daly and others, 2008]; and MTBS fire data [Eidenshink and others, 2007]) often lags behind the availability of lek count data, which could inhibit real-time applications of the early warning system. In the absence of computational and data-driven restrictions, our pattern-seeking hierarchical model structure and rules for the evaluation process can be built into the back-end of a user-friendly computer interface. With slow and fast thresholds already established and cluster scales of interest delineated, resource managers could then easily input annual lek count data and obtain real-time results for their populations and specific questions. Covariate associations can then be evaluated in a post hoc fashion through GIS overlays of available land cover and disturbance, ground-truthing, or more formal modeling. In addition, although cluster and threshold delineations are computationally complex and would need to be quantified for other parts of the sage-grouse range, the evaluation process built into a user-friendly interface lends itself well to future range-wide applications.

The hierarchical framework we developed can be modified to allow higher resolution detection of local population units that are declining and decoupling by incorporating additional finer scale clusters for contrast against higher scales. The rules presented within our analysis are relatively coarse, whereby only two spatial scales were used to represent local scale effects (those to leks and neighborhoods) and contrasted against one single larger spatial scale to represent patterns driven by climatic factors. However, the clustering process also delineated clusters scales 1 and 3 or 4 that differed significantly from cluster scale 5 (the climate scale) in terms of lower estimates of population closure (fig. 12). Using more spatial scales in this framework can help link the scale of habitat disturbances to affected populations. The sequence of contrasts would be identical to those illustrated in fig. 10, except in this case, other larger scales that might represent declines by more localized factors (for example cluster scale 3) is first contrasted against the climate scale. If it decouples, the next lowest local scale (in this case, cluster scale 2) is contrasted against the climate scale. If scale 2 does not decouple, the process stops at scale 3. If scale 2 does decouple, the process repeats itself until all successive lower scales (scale 1 to individual lek) are contrasted. Moreover, if the largest local scale does not decouple, all-lower-order scales are sequentially contrasted until all scales are exhausted. The same rationale could be applied for adding more clusters representative of climate effects (for example, scales 6 and 7), in the event a singular climate scale cluster (currently set at scale 5) decouples from regional-scale trends. Importantly, slow and fast thresholds for decoupling would first need to be estimated for each cluster scale to use these approaches. Nevertheless, our four-scale (for example, scales were individual leks, cluster scale 2 [neighborhood], cluster scale 5 [climate], and regional) evaluation is simplified, yet

derived using a combination of quantitative evidence of sage-grouse migration between leks, biological relevance regarding sage-grouse populations connection or lack-there-of between population units, and management practicality derived from a stakeholder process.

The evaluation process focused on identifying populations exhibiting slow and steady decline, or at risk of outright extirpation. However, the rules of the evaluation process can be modified to indicate other types of trends relevant to management. For example, instances can develop where local populations are stable or increasing slightly, but nevertheless are underperforming compared to rapidly growing populations measured at the climate scale (for example, fig. 9*B*). In this case, local factors may be suppressing expected higher rates of population growth, and this type of decoupling could be identified with the same type of retrospective simulation analyses described previously. Thresholds can also be modified to identify when local populations are outperforming larger surrounding populations. This could be a particularly important threshold that could help demonstrate where, and to what extent, restoration efforts are positively affecting local populations of sage-grouse. These possible applications illustrate how our example framework to identify declining populations is just one of many that can be applied once question-specific thresholds and corresponding rules are calculated and validated. Hence, our framework can allow identification of sage-grouse populations responding positively to management as well as those that indicate the need for possible intervention.

Warning System Patterns for 2016

Our final objective was to describe population status and report soft and hard signals at multiple spatial scales of sage-grouse in northeastern California and Nevada as of 2016. Notably, results indicate that sage-grouse populations in this region have declined by an average of 3.86 percent annually over the last 17 years. This estimated rate of decline corresponds to other estimates of relative declining trends documented for sage-grouse in the Great Basin over long time periods (Garton and others, 2011; Coates, Ricca, and others, 2016). When we simulated management actions activated under different combinations of successive slow and fast warnings and with progressively decreasing efficiency, nearly all outcomes reflected a relative slowing (rather than cessation) of population declines across the region over the following 17 years (tables 3 and 4). However, our simulations indicated that the selected temporal threshold of 3 out of 4 consecutive years of slow warnings or 2 out 3 consecutive years of fast warnings could reverse negative trends and bring the entire region to stability if all implemented management actions are 100 percent effective. Although 100 percent effectiveness is a rather unrealistic scenario (see section, “Caveats”), management actions implemented under our example rules for activating a hard signal that are only 50 percent effective may still cut the long-term rates of annual population decline across the region by one-half. Alternatively, waiting too long to activate a hard signal may limit manager’s ability to slow the current rate of region-wide decline.

Overall, our results indicate that the Ely climate cluster had the largest number of leks in decline based on our soft signal criteria. Additionally, the largest number of neighborhood leks meeting the criteria for a soft signal were located in the Ely climate cluster. However, the Ely climate cluster did not signal, which suggests that lek and neighborhood cluster declines were driven by local factors and not larger scale climatic variation. In contrast, hard signals were constrained to leks only, and post hoc analyses are necessary to begin identification of local perturbations that may be linked to these rapidly declining populations.

Caveats

We present five caveats for consideration when interpreting or implementing the example framework and early warning system. First, although an advantage of state-space models is their ability to estimate missing count data based on prior variance of observed counts, they require adequate count data to inform estimates whereby minimal data gaps or sharing of information across leks using hyper-parameters (that is, the automatic selection of smoothing parameters) increase the reliability of parameter estimates within state-space models (Kery and Schaub, 2012). The reliability of estimates derived via state-space models would be enhanced by standardized lek count protocols that minimize the number of years between counts that allow for improved parameter estimation. Our framework can be modified to work with other models, such as N-mixture models that take advantage of information from repeated intra-annual counts (Royle, 2004) rather than maximum annual lek-count data, which allows another means of estimating observation error and detection probabilities that can vary across space (leks) and time (year and time sampled) (Monroe and others, 2016; Fremgen and others, 2017). Repeated counts conducted within a season can also confound detection probability (that is, miscounting sage-grouse that are available to count) with variation in visitation rates (that is, not all sage-grouse at any point in time are available to count). However, recent advances using dynamic N-mixture models (Dail and Madsen, 2011) that relax assumptions of closure may prove useful. We chose state-space models and used the maximum lek count largely because our dataset did not report repeated counts of leks within seasons. Improvements to this population estimation framework could involve incorporation of repeated count data combined with information on lek visitation rates, which could be conducted and reported.

Second, we did not explicitly partition density-dependent from density-independent effects within and among spatial scales. Weak density-dependent feedbacks contribute to population stability (May, 1974; Ahrestani and others, 2016), whereas density-independent factors can contribute to positive or negative population dynamics (Saether, 1997; Ahrestani and others, 2016). Our lack of accounting for these effects that contribute to annual variation in sage-grouse abundance within and among spatial scales (Blomberg and others, 2017, falls in the same category as our lack of accounting for spatially explicit environmental covariates. Our goal was to develop an early warning system that identified pattern rather than mechanisms at different spatial scales across a broad geographic extent. The system does not allow for identification of specific effects related to demographic and environmental stochasticity. Thus, results should be evaluated in terms of different smaller compared to larger scale patterns without assuming specific causes.

Third, we assumed that simulated management actions had uniform effectiveness based on the intensity of application (that is, 100 percent management intensity would neutralize 100 percent of all hard signals, 90 percent management intensity would neutralize 90 percent of all hard signals, and so forth). In reality, the effectiveness of management actions aimed at restoring habitat conditions for sage-grouse is highly variable and dependent on factors such as underlying conditions influencing resilience to disturbance and resistance to invasion, how degraded a site has become (that is, whether or not it has crossed a state-transition), the type of disturbance experienced, the type of management action or restoration technique implemented, and the abiotic conditions at the time management actions are implemented (Arkle and others, 2014; Chambers and others, 2014; Pyke and others, 2015; Pilliod and others, 2017). Hence, our estimates of effectiveness should be viewed as relative and not absolute measures.

Fourth, we assumed that delineations in cluster scale 5 represented sage-grouse populations that experienced different climatic influences. This is justified in part by the inclusion of precipitation and temperature indices as environmental covariates in the cluster delineation modeling. These delineations match reasonably well with large-scale gradients of variation in precipitation and temperature, and corresponding mesic sagebrush steppe ecosystems in the more northern clusters and xeric Great Basin sagebrush ecosystems in the more southern clusters (Coates, Casazza, and others, 2016). Nevertheless, climate effects can cross scale boundaries and become hard to separate from localized surface-disturbance effects. For example, broad-scale drought could exert different influences on sage-grouse populations inhabiting neighborhood clusters nested within more xeric regions that may be less resilient to drought than those nested within more mesic regions because springs and seeps that dry-up in xeric regions are likely more limiting to sage-grouse populations compared to those in mesic regions.

Fifth, although it is possible that effects at smaller spatial scales driven by local-scale factors vary based on larger-scale climatic impacts, our framework is sensitive to identifying where and when local effects occur regardless of their dependency on climatic effects. Post hoc evaluations that identify causes of local-scale declines may tease apart relationships between local disturbances and larger-scale climatic effects, and these additional investigations are necessary to inform the type and timing of appropriate management actions.

Conclusion

In conclusion, the example early warning system we describe in this report can be a powerful and flexible management tool that allows for separation of population trends occurring as a result of local and more manageable stressors, relative to those occurring at broader scales. Built-in spatial and temporal thresholds help guard against implementing unnecessary management action for populations that falsely signal a warning. Simulations using management action implemented once populations begin to decline precipitously indicate that the early warning system can help slow overall population declines. This framework can be a useful tool for managing sage-grouse populations and their habitats in the Great Basin and can be expanded to assist rangewide applications.

References Cited

Ahrestani, F.S., Smith, W.K., Hebblewhite, M., Running, S., and Post, E., 2016, Variation in stability of elk and red deer populations with abiotic and biotic factors at the species distribution scale: Ecology, v. 97, p. 3,184–3,194.

Aldridge, C.L., and Boyce, M.S., 2007, Linking occurrence and fitness to persistence—a habitat-based approach for endangered greater sage-grouse: Ecological Applications, v. 17, p. 508–526.

Aldridge, C.L., Nielsen, S.E., Beyer, H.L., Boyce, M.S., Connelly, J.W., Knick, S.T., and Schroeder, M.A., 2008, Range-wide patterns of greater sage-grouse persistence: Diversity and Distributions, v. 14, p. 983–994.

Anderson, J.E., and Holte, K.E., 1981, Vegetation development over 25 years without grazing on sagebrush-dominated rangeland in southeastern Idaho: Journal of Range Management, v. 34, p. 25–29.

Arkle, R.S., Pilliod, D.S., Hanser, S.E., Brooks, M.L., Chambers, J.C., Grace, J.B., Knutson, K.C., Pyke, D.A., Welty, J.L., and Wirth, T.A., 2014, Quantifying restoration effectiveness using multi-scale habitat models: implications for sage-grouse in the Great Basin: Ecosphere, v. 5, issue 3, article 31.

AssunÇão, R.M., Neves, M.C., Câmara, G., and Da Costa Freitas, C., 2006, Efficient regionalization techniques for socio-economic geographical units using minimum spanning trees: International Journal of Geographical Information Science, v. 20, p. 797–811.
Beck, J.L., and Mitchell, D.L., 2000, Influences of livestock grazing on sage grouse habitat: Wildlife Society Bulletin, v. 28, p. 993–1002.
Bissonette, J., 1997, Scale sensitive ecological properties—Historical context, current meaning, *in* Bissonette, J., ed., Wildlife and landscape ecology—Effects of pattern and scale: New York, New York, Springer-Verlag, p. 3–31.
Bissonette, J.A., 2016, Avoiding the scale sampling problem—A consistent solution: Journal of Wildlife Management, v. 80, p. 192–205.
Bivand, R., and Piras, C., 2015, Comparing implementations of estimation methods for spatial econometrics: Journal of Statistical Software, v. 63, p. 1–36.
Bivand, R.S., Hauke, J., and Kossowski, T., 2013, Computing the Jacobian in Gaussian spatial autoregressive models—An illustrated comparison of available methods: Geographical Analysis, v. 45, p. 150–179.
Blackburn, W.H., and Tueller, P.T., 1970, Pinyon and juniper invasion in black sagebrush communities in east-central Nevada: Ecology, v. 51, p. 841–848.
Blomberg, E.J., Sedinger, J.S., Atamian, M.T., and Nonne, D.V., 2012, Characteristics of climate and landscape disturbance influence the dynamics of greater sage-grouse populations: Ecosphere, v. 3, issue 6, article 55.
Blomberg, E.J., Gibson, D., Atamian, M.T., and Sedinger, J.S., 2017, Variable drivers of primary versus secondary nesting; density-dependence and drought effects on greater sage-grouse: Journal of Avian Biology, v. 48, no. 6, p. 827–836, doi:10.1111/jav.0098.
Bradley, B.A., 2010, Assessing ecosystem threats from global and regional change—Hierarchical modeling of risk to sagebrush ecosystems from climate change, land use and invasive species in Nevada, USA: Ecography, v. 33, p. 198–208.
Bureau of Land Management, 2015, Notice of availability of the record of decision and approved resource management plan amendments for the Great Basin region greater sage-grouse sub-regions of Idaho and Southwestern Montana; Nevada and Northeastern California; Oregon; and Utah: Federal Register, v. 80, no. 185, p. 57,633–57,635, accessed June 30, 2017, at https://www.gpo.gov/fdsys/pkg/FR-2015-09-24/pdf/2015-24213.pdf.
Burnham, K.P., and Anderson, D.R., 2002, Model selection and multimodel inference (2nd ed.): New York, New York. Springer-Verlag, 488 p.
Chambers, J.C., Bradley, B.A., Brown, C.S., D'Antonio, C., Germino, M.J., Grace, J.B., Hardegree, S.P., Miller, R.F., and Pyke, D.A., 2014, Resilience to stress and disturbance, and resistance to *Bromus tectorum* L. invasion in cold desert shrublands of Western North America: Ecosystems, v. 17, p. 360–375.
Clark, J., 2007, Models for ecological data (1st ed.): Princeton, New Jersey, Princeton University Press, 152 p.
Coates, P.S., and Delehanty, D.J., 2010, Nest predation of greater sage-grouse in relation to microhabitat factors and predators: Journal of Wildlife Management, v. 74, p. 240–248.
Coates, P.S., Casazza, M.L., Blomberg, E.J., Gardner, S.C., Espinosa, S.P., Yee, J.L., Wiechman, L., and Halstead, B.J., 2013, Evaluating greater sage-grouse seasonal space use relative to leks—Implications for surface use designations in sagebrush ecosystems: The Journal of Wildlife Management, v. 77, p. 1,598–1,609.

Coates, P.S., Halstead, B.J., Blomberg, E.J., Brussee, B.E., Howe, K.B., Wiechman, L., Tebbenkamp, J., Reese, K.P., Gardner, S.C., and Casazza, M.L., 2014, A hierarchical integrated population model for greater sage-grouse (*Centrocercus urophasianus*) in the Bi-State Distinct Population Segment, California and Nevada: U.S. Geological Survey Open-File Report 2014-1165, 34 p., https://dx.doi.org/10.3133/ofr20141165.

Coates, P.S., Casazza, M.L. Brussee, B.E., Ricca, M.A., Gustafson, K.B. Sanchez-Chopitea, E. Mauch, K., Neill, L. Gardner, S.C., Espinosa, S.P., and Delehanty, D.J., 2016, Spatially explicit modeling of annual and seasonal habitat for greater sage-grouse (Centrocercus urophasianus) in Nevada and Northeastern California—An updated decision-support tool for management: U.S. Geological Survey Open-File Report 2016-1080, 84 p., https://pubs.er.usgs.gov/publication/ofr20161080.

Coates, P.S., Ricca, M.A., Prochazka, B.G., Brooks, M.L., Doherty, K.E., Kroger, T., Blomberg, E.J., Hagen, C.A., and Casazza, M.L., 2016, Wildfire, climate, and invasive grass interactions negatively impact an indicator species by reshaping sagebrush ecosystems: Proceedings of the National Academy of Sciences, v. 113, p. 12,745–12,750.

Cross, T.B., Naugle, D.E., Carlson, J.C., and Schwartz, M.K., 2016, Hierarchical population structure in greater sage-grouse provides insight into management boundary delineation: Conservation Genetics, v. 17, p. 1,417–1,433.

Cumming, G., Cumming, D.H., and Redman, C., 2006, Scale mismatches in social-ecological systems—Causes, consequences, and solutions: Ecology and Society, v. 11, issue 1, article 14.

Dahlgren, D.K., Guttery, M.R., Messmer, T.A., Caudill, D., Dwayne Elmore, R., Chi, R., and Koons, D.N., 2016, Evaluating vital rate contributions to greater sage-grouse population dynamics to inform conservation: Ecosphere, v. 7. issue 3, article e01249.

Dail, D., and Madsen, L., 2011, Models for estimating abundance from repeated counts of an open metapopulation: Biometrics, v. 67, p. 577–587.

Daly, C., Halbleib, M., Smith, J.I., Gibson, W.P., Doggett, M.K., Taylor, G.H., Curtis, J., and Pasteris, P.P., 2008, Physiographically sensitive mapping of climatological temperature and precipitation across the conterminous United States: International Journal of Climatology, v. 28, p. 2,031–2,064.

Davies, K.W., Boyd, C.S., Beck, J.L., Bates, J.D., Svejcar, T.J., and Gregg, M.A., 2011, Saving the sagebrush sea—An ecosystem conservation plan for big sagebrush plant communities. Biological Conservation, v. 144, p. 2,573–2,584.

Doherty, K.E., Naugle, D.E., Walker, B.L., Graham, J.M., 2008, Greater sage-grouse winter habitat selection and energy development: Journal of Wildlife Management, v. 72, p. 187–195.

Eidenshink, J., Schwind, B., Brewer, K., Zhu, Z.L., Quayle, B., and Howard, S., 2007, A project for monitoring trends in burn severity: Fire Ecology, v. 3, p. 3–22.

Epifanio, J., 2000, The Status of coldwater fishery management in the United States—An overview of state programs: Fisheries, v. 25, p. 13–27.

Environmental Systems Research Institute, Inc. (ESRI), 2011, ArcGIS Desktop—Release 10.3.1: Redlands, California, Environmental Systems Research Institute.

Fedy, B.C., and Aldridge, C.L., 2011, The importance of within-year repeated counts and the influence of scale on long-term monitoring of sage-grouse: Journal of Wildlife Management, v. 75, p. 1,022–1,033.

Fedy, B.C., and Doherty, K.E., 2011, Population cycles are highly correlated over long time series and large spatial scales in two unrelated species—Greater sage-grouse and cottontail rabbits: Oecologia, v. 165, p. 915–924.

Fedy, B.C., Doherty, K.E., Aldridge, C.L., O'Donnell, M., Beck, J.L., Bedrosian, B., Gummer, D., Holloran, M.J., Johnson, G.D., Kaczor, N.W., Kirol, C.P., Mandich, C.A., Marshall, D., Mckee, G., and others, 2014, Habitat prioritization across large landscapes, multiple seasons, and novel areas—An example using greater sage-grouse in Wyoming: Wildlife Monographs, v. 190, p. 1–39.

Fremgen, A.L., Rota, C.T., Hansen, C.P., Rumble, M.A., Gamo, R.S., and Millspaugh, J.J., 2017, Male greater sage-grouse movements among leks: The Journal of Wildlife Management, v. 81, p. 498–508.

Fuhlendorf, S.D., Woodward, A.J.W., Leslie, D.M., and Shackford, J.S., 2002, Multi-scale effects of habitat loss and fragmentation on lesser prairie-chicken populations of the U.S. Southern Great Plains: Landscape Ecology, v. 17, p. 617–628.

Garton, E.O., Connelly, J.W., Horne, J.S., Hagen, C.A., Moser, A.M., and Schroeder, M.A., 2011, Greater sage-grouse population dynamics and probability of persistence, *in* Knick, S.T., and Connelly, J.W., eds., Greater sage-grouse—Ecology and conservation of a landscape species and its habitats—Studies in avian biology: Berkeley, University of California Press, p. 293–381.

Garton, E.O., Wells, A.G., Baumgardt, J.A., and Connelly, J.W., 2015, Greater sage-grouse population dynamics and probability of persistence: Final Report to Pew Charitable Trusts, 90 p.

Gelman, A., Carlin, J.B., Stern, H.S., and Rubin, D.B., 2004, Bayesian data analysis (2nd ed.): Boca Raton, Florida, Chapman and Hall/CRC, 690 p.

Green, A.W., Aldridge, C.L., and O'Donnell, M.S., 2017, Investigating impacts of oil and gas development on greater sage-grouse: Journal of Wildlife Management, v. 81, p. 46–57.

Gregg, M.A., and Crawford, J.A., 2007, Survival of greater sage-grouse chicks and broods in the northern Great Basin: Journal of Wildlife Management, v. 73, p. 904–913.

Germino, M.J., Chambers, J.C., Brown, C.S., eds., 2016, Exotic brome-grasses in arid and semiarid ecosystems of the western US—Causes, consequences, and management implications: Switzerland, Springer International Publishing, 475 p.

Hanser, S.E., and Knick, S.T., 2011, Greater sage-grouse as an umbrella species for shrubland birds—a multi-scale assessment, *in* Knick. S.T., and Connelly, J.W., eds., Greater sage-grouse—Ecology and conservation of a landscape species and its habitats—Studies in Avian Biology, University of California Press, p. 475–487.

Hobbs, N.T., and Hooten, M.B., 2015, Bayesian models (1st ed.): Princeton, New Jersey, Princeton University Press, 320 p.

Kery, M., and Schaub, M., 2012, Bayesian population analysis using WinBUGS—A hierarchical perspective (1st ed.): San Diego, California, Academic Press, 554 p.

Knick, S.T., Hanser, S.E., and Preston, K.L., 2013, Modeling ecological minimum requirements for distribution of greater sage-grouse leks—Implications for population connectivity across their western range, U.S.A: Ecology and Evolution, v. 3, no. 6, p. 1,539–1,551.

Levin, S.A., 1992, The problem with scale and pattern in ecology: Ecology, v. 73, p. 1,943–1,967.

Lindenmayer, D.B., and Likens, G.E., 2010, The science and application of ecological monitoring: Biological Conservation, v. 143, p. 1,317–1,328.

Lindstrom, J., Ranta, E., and Linden, H., 1996, Large-scale synchrony in the dynamics of capercaillie, black grouse and hazel grouse populations in Finland: Oikos, v. 76, p. 221–227.

Lu, B., 2014, shp2graph package—Convert a SpatialLinesDataFrame object to a "igraph-class" object: R package version 0-2, The Comprehensive R Archive Network Web site, accessed August 25, 2016, at https://CRAN.R-project.org/package=shp2graph.

May, R.M., 1974., Biological populations with nonoverlapping generations: stable points, stable cycles, and chaos: Science, v. 186, p. 645–647.

McCaffery, R., and Lukacs, P.M., 2016, A generalized integrated population model to estimate greater sage-grouse population dynamics: Ecosphere, v. 7, issue 11, article e01585.
Miller, R.F., and Rose, J.A., 1999, Fire history and western juniper encroachment in sagebrush steppe: Journal of Rangeland Management, v. 52, p. 550–559.
Miller, R.F., Knick, S.T., Pyke, D.A., Meinke, C.W., Hanser, S.E., Wisdom, M.J., and Hild, A.L., 2011, Characteristics of sagebrush habitats and limitations to long-term conservation, in Knick, S.T., and Connelly, J.W., eds., Greater sage-grouse—Ecology and conservation of a landscape species and its habitats: Berkeley, University of California Press, Studies in Avian Biology, no. 38, p. 145–184.
Monroe, A.P., Edmunds, D.R., and Aldridge, C.L., 2016, Effects of lek count protocols on greater sage-grouse population trend estimates: The Journal of Wildlife Management, v. 80, p. 667–678.
Monroe, A.P., Aldridge, C.L., Assal, T.J., Veblen, K.E., Pyke, D.A., and Casazza, M.L., 2017, Patterns in Greater Sage-grouse population dynamics correspond with public grazing records at broad scales: Ecological Applications, v. 27, p. 1,096–1,107.
Morris, W.F., and Doak, D.F., 2002, Quantitative conservation biology (4th ed.): Sunderland, MA, Sinauer Associates Inc., 480 p.
Moynahan, B.J., Lindberg, M.S., and Thomas, J.W., 2006, Factors contributing to process variance in annual survival of female greater sage-grouse in Montana: Ecological Applications, v. 16, p. 1,529–1,538.
Oakley, K.L., Thomas, L.P., and Fancy, S.G., 2003, Guidelines for long-term monitoring protocols: Wildlife Society Bulletin, v. 31, p. 1,000–1,003.
O'Donnell, M.S., and Ignizio, D.A., 2012, Bioclimatic predictors for supporting ecological applications in the conterminous United States: U.S. Geological Survey Data Series 691, 10 p., https://pubs.usgs.gov/ds/691/ds691.pdf.
Pilliod, D.S., Welty, J.L., and Toevs, G.R., 2017, Seventy-five years of vegetation treatments on public rangelands in the Great Basin of North America: Rangelands, v. 39, p. 1–9.
Plummer, M., Stukalov, A., and Denwood, M., 2015, Bayesian graphical models using MCMC, R package 'rjags', version 3-15: The Comprehensive R Archive Network Web site, http://cran.r-project.org/web/packages/rjags/rjags.pdf.
Pollock, K.H., Nichols, J.D., Simons, T.R., Farnsworth, G.L., Bailey, L.L., and Sauer, J.R., 2002, Large scale wildlife monitoring studies—Statistical methods for design and analysis: Environmetrics, v. 13, p. 105–119.
Pyke, D.A., Chambers, J.C., Pellant, M., Knick, S.T., Miller, R,F., Beck, J.L., Doescher, P.S., Schupp, E.W., Roundy, B.A., Brunson, M., and McIver, J.D., 2015, Restoration handbook for sagebrush steppe ecosystems with emphasis on greater sage-grouse habitat—Part 1. Concepts for understanding and applying restoration: U.S. Geological Survey Circular 1416, 44 p., https://dx.doi.org/10.3133/cir1416.
R Core Team, 2016, R: A language and environment for statistical computing: Vienna, Austria, R Foundation for Statistical Computing, Web site, accessed August 25, 2016, at https://www.R-project.org/.
Ranta, E., Kaitala, V., Lindstrom, J., and Linden, H., 1995, Synchrony in population dynamics—Proceedings of the Royal Society of London B: Biological Sciences, v. 262, p. 113–118.
Riley, S.J., DeGloria, S.D., and Elliot, R., 1999, A terrain ruggedness index that quantifies topographic heterogeneity: Intermountain Journal of Sciences, v. 5, p. 23–27.
Rich, T., 1985, Sage-grouse population fluctuations—Evidence for a 10-year cycle: Idaho State Office, Bureau of Land Management, Technical Bulletin, no. 85-1, 34 p.
Rich, T., and Altman, B., 2001, Under the sage-grouse umbrella: Bird Conservation, v. 14, no. 10.

Rich, T.D., Wisdom, M.J., and Saab, V.A., 2005, Conservation of sagebrush steppe birds in the interior Columbia Basin,. *in* Ralph, C.J., Rich, R., Long, L., eds., Proceedings of the Third International Partners in Flight Conference: U.S. Department of Agriculture, Albany, California, Forest Service, Pacific Southwest Research Station, General Technical Report PSW-GTR-191, p. 589–606.

Rowland, M. M., Wisdom, M.J., Suring, L.H., and Meinke, C.W., 2006, Greater sage-grouse as an umbrella species for sagebrush-associated vertebrates: Biological Conservation, v. 129, p. 323–335.

Royle, J.A., 2004, N-mixture models for estimating population size from spatially replicated counts; Biometrics, v. 60, p. 108–115.

Sadoul, N., 1997, The importance of spatial scales in long-term monitoring of colonial Charadriiformes in Southern France: Colonial Waterbirds, v. 20, p. 330–338.

Saether, B.E., 1997, Environmental stochasticity and population dynamics of large herbivores: A search for mechanisms: Trends in Ecology & Evolution, v. 12, p. 143–149.

Sappington, J.M., Longshore, K.M., and Thompson, D.B., 2007, Quantifying landscape ruggedness for animal habitat analysis—A case study using bighorn sheep in the Mojave Desert: The Journal of Wildlife Management, v. 71, p. 1,419–1,426.

Schroeder, M.A., Aldridge, C.L., Apa, A.D., Bohne, J.R., Braun, C.E., Bunnell, S.D., Connelly, J.W., Deibert, P.A., Gardner, S.C., Hilliard, M.A., Kobriger, G.D., McAdam, S.M., McCarthy, C.W., McCarthy, J.J., Mitchell, D.L., Rickerson, E.V., and Stiver, S.J., 2004, Distribution of sage-grouse in North America: Condor, v. 106, p. 363–376.

Schroeder, M.A., 1997, Unusually high reproductive effort by sage grouse in a fragmented habitat in north-central Washington: Condor, v. 99, p. 933–941.

Suring, L.H., Wisdom, M.J., Tausch, R.J., Miller, R.F., Rowland, M.M., Schueck, L., and Meinke, C.W., 2005, Modeling threats to sagebrush and other shrubland communities, *in*, Habitat threats in the sagebrush ecosystem: Lawrence, Kansas, Alliance Communications Group, p. 114–149.U.S. Fish and Wildlife Service, 2015, Endangered and threatened wildlife and plants—12-month finding on a petition to list greater sage-grouse (*Centrocercus urophasianus*) as an endangered or threatened species: Federal Register, v. 80, no. 191, p. 59,858–59,942, accessed June 30, 2017, at https://www.gpo.gov/fdsys/pkg/FR-2015-10-02/pdf/2015-24292.pdf.

Western Association of Fish and Wildlife Agencies, 2015, Greater sage-grouse population trends—An analysis of lek count databases 1965–2015: Western Association of Fish and Wildlife Agencies Web site, accessed August 2015, at http://www.wafwa.org/Documents%20and%20Settings/37/Site%20Documents/News/Lek%20Trend%20Analysis%20final%208-14-15.pdf.

Walker, B.L., Naugle, D.E., and Doherty, K.E., 2007, Greater sage-grouse population response to energy development and habitat loss: Journal of Wildlife Management, v. 71, p. 2,644–2,654.

Wallace, B.P., DiMatteo, A.D., Hurley, B.J., Finkbeiner, E.M., Bolten, A.B., Chaloupka, M.Y., Hutchinson, B.J., Abreu-Grobois, F.A., Amorocho, D., Bjorndal, K.A., Bourjea, J., Bowen, B.W., Dueñas, R.B., Casale, P., Choudhury, B.C., Costa, A., Dutton, P.H., Fallabrino, A., Girard, A., Girondot, M., Godfrey, M.H., Hamann, M., López-Mendilaharsu, M., Marcovaldi, M.A., Mortimer, J.A., Musick, J.A., Nel, R., Pilcher, N.J., Seminoff, J.A., Troëng, S., Witherington, B., and Mast, R.B., 2010, Regional management units for marine turtles—A novel framework for prioritizing conservation and research across multiple scales: PloS one, v. 5, no. 12, e15465.

Xian, G., Homer, C., Meyer, D., and Granneman, B., 2013, An approach for characterizing the distribution of shrubland ecosystem components as continuous fields as part of NLCD: ISPRS Journal of Photogrammetry and Remote Sensing, v. 86, p. 136–149.

Publishing support provided by the U.S. Geological Survey
Science Publishing Network, Tacoma Publishing Service Center

For more information concerning the research in this report, contact the
Director, Western Ecological Research Center
U.S. Geological Survey
3020 State University Drive East
Sacramento, California 95819
https://www.werc.usgs.gov/

ISSN 2331-1258 (online)
https://doi.org/10.3133/ofr20171089